UNIVERSIDADE DE LISBOA
FACULDADE DE CIÊNCIAS
DEPARTAMENTO DE QUÍMICA E BIOQUÍMICA

Molecular Studies of Alpha-Synuclein Aggregation

Luís Maria Mongiardim Palmares

Mestrado em Bioquímica
Especialização em Bioquímica Médica

Dissertação orientada por:
Prof. Doutor Tiago F. Outeiro
Prof. Doutor Cláudio M. Gomes

2020

Acknowledgements

First and foremost, I would like to thank Professor Tiago Outeiro for giving me the amazing opportunity to go to work abroad on my thesis, helping me expand my knowledge of the world and guiding me on my first steps as a scientist. I would also like to thank Prof. Cláudio Gomes for the help he gave in choosing an Erasmus+ dissertation and for the assistance given during it.

To all my colleagues in the Outeiro lab group I would like to express my gratitude for everything you teached and helped me with ever since I first arrived there.

To Christiane Fahlbusch, Daniela Proto, Sonja Reisenauer and Diana Lázaro for helping me get started and teaching me the ins and outs of the workplace.

To Renato Domingues, Inês Brás, Liana Shvachiy, and Manuel Leon for all the advice and company they gave me during my first time living abroad, helping me to become more independent**.**

To Patrícia Santos I give a special thanks for the guidance she gave me in every step of my work, and for always being there for me whenever I had doubts or faced roadblocks. Without your kindness, sincerity, and understanding, I would not be the scientist I am today.

I would also like to express my gratitude to my friends and family who supported me during this last year.

To my friends Francisco Traquete and João Ferreira, who were always there to help answer the questions for which I was too embarrassed to ask anyone else, and for keeping in touch on a daily basis the entire time I was living abroad

And to my cousins José Maria Monteiro and Xavier Mascarenhas for the hour-long phone conversations we'd have while living in separate countries, and for always making the best of the trips I made to Portugal during this year.

To my siblings Francisca Palmares and Duarte Palmares, and my parents Luís Palmares and Filipa Palmares, for not only supporting me in this year long journey, but also the rest of my life. Constantly showing concern for how I was, and for always showing excitement whenever I made a trip home.

Resumo

A doença de Parkinson (DP) e Demência com Corpos de Lewy são duas das doenças neurodegenerativas mais comuns que afetam o ser humano. Muitos estudos já foram feitos para aumentar o conhecimento existente das doenças mas continua a haver um longo caminho pela frente até ser possível por um fim às patologias. Estas patologias têm em comum a caracteristica histopatologica da presença de Corpos de Lewy (CL), que são inclusões grandes compostas maioritariamente pela proteina alfa-sinucleína (ASYN) e por diversos outros componentes das células, fazendo parte do seu próprio grupo de doenças denominado "Sinucleinopatias".

O foco principal deste projeto envolve a utilização dos modelos de transfeção de uma proteína de ASYN que possui EGFP truncado no seu C-terminal (SynT), e modelos de transfeção de complementação bimolecular da fluorescência (BiFC) onde são transfetadas duas proteínas (iguais ou diferentes) com cada a possuir uma parte diferente da proteína venus que recupera a sua fluorescência na interação entre proteínas com duas partes diferentes da venus. Estes modelos permitem o estudo da oligomerização de ASYN (BiFC) e de grandes inclusões de ASYN que se assemelham com CL (BiFC e SynT). Um dos maiores objectivos deste projeto é a observação destas inclusões com a utilização de técnicas de microscopia de super-resolução, denominadamente stimulated emission depletion (STED) e microscopia de expansão (ExM) X10. Enquanto que STED já é uma técnica utilizada há mais de 20 anos, X10 ExM é uma técnica relativamente recente, tendo sido primeiro publicada em 2018 e sendo uma adaptação da técnica de microscopia de expansão que foi proposta em 2015. Assim a técnica de X10 ExM ainda é pouco utilizada, não existindo, do meu conhecimento, quaisqueres artigos publicados sobre o uso da técnica relativamente a ASYN ou PD em geral. Tendo em conta a novidade que é a técnica de X10 ExM espero conseguir demonstrar através deste projeto o potencial que a técnica tem para não só o estudo de CL como também sendo uma técnica de microscopia de super-resolução que consegue alcançar as resoluções altas de outras técnicas topo-de-linha, ultrapassando a barreira que o limite da difração impõe sobre as resoluções obtidas em microscópios convencionais. Ao mesmo tempo, X10 ExM é bastante accessível em termos dos custos e equipamento necessário, com a técnica possibilitando a obtenção destas altas resoluções em microscópios de fluorescência convencionais, visto que o processo da técnica envolve só a manipulação das amostras em sí, expandindo as amostras até à volta de 10× em todas as dimensões.

Através do uso da técnica X10 ExM em modelos de células H4 transfetadas com modelos de SynT e BiFC foi possível observar observar a ASYN com grande detalhe em comparação às células pre-expansão. Nestas células consegue-se observar o ASYN livre no citoplasma das células com uma distribuição muito mais claramente pontuada, semelhante ao que se observa por microscopia de STED, em comparação ao fundo vermelho difuso que se observa muitas vezes nestas células sem ExM. Também foi possível observar inclusões de ASYN presentes nestas células que aparentam possuir uma estrutura heterogénea, algo que as aproxima da estrutura de CL.

De forma a conseguir estudar melhor a heterogeneidade destas inclusões foram feitos estudos de co-localização das inclusões com outras proteínas, das quais já são conhecidas por fazerem parte da composição dos LB, utilizando a técnica de X10 ExM. Infelizmente a utilização desta técnica trouxe uns certos problemas, onde devido ao uso de um passo de digestão que põe as amostras em contacto com Proteanase K, os anticorpos utilizados nessas proteínas acabaram por perder toda ou quase toda a sua fluorescência, impossibilitando o estudo da sua co-localização com ASYN. Devido a este problema o estudo da co-localização ficou limitado às imagens obtidas pre-expansão das células, que pelo menos confirma que todas as proteínas co-localização com estas inclusões (com a exceção de uma das proteínas que no entanto já é confirmado por diversas literaturas como fazendo parte dos CL). Resolver o

problema da perda de fluorescência fica assim uma via futura muito importante, podendo ser resolvida por modificações no procedimento como o aumento da concentração de anticorpos utilizados, um passo de "anchoring" das amostras prolongado, adicionar um passo de recuperação dos antigénios, ou até mesmo passar a aplicar a immunocoloração das amostras já depois destas estarem expandidas, embora esta ultíma possível solução pode trazer problemas em relação ao estado desconhecido em que os antigénios se encontram após o procedimento de X10 ExM.

A outra técnica de microscopia de super-resolução praticada foi o STED, uma técnica que, ao contrário de muitas outras de microscopia de super-resolução, não precisa de passos de análise da imagem obtida que envolvem a aplicação de modelos matemáticos e software para o melhoramento da resolução. Em vez disso STED funciona pela utilização de um raio STED que é lançado para a amostra numa aréa com forma de donut a envolver o raio de excitação. O contacto de fluoróforos com o raio STED leva a que a sua fluorescência seja esgota, o que essencialmente leva a que a separação do sinal de diferentes fluóroforos seja facilitada. Ao utilizar esta técnica com células transfetadas com modelos de SynT foi possivél obter imagens com qualidade elevada, embora alguma optimização da técnica será necessaria para conseguir usufruir do seu potencial completo, e o fotobranqueamento causado pelo uso repetido do raio STED pode trazer algumas dificuldades na análise de inclusões especificas nas células. Mas mesmo assim esta técnica ainda demonstra ser muito vantajosa para o estudo destas inclusões heterogéneas. Uma ferramenta que também foi experimentada com este microscópio foi a escolha do plano em que as imagens são obtidas, algo que permite um estudo mais tri-dimensional da estrutura das inclusões.

Possiveís vias futuras que podem ser exploradas seriam a combinação da técnica de X10 ExM com várias outras técnicas de microscopia de super-resolução, como STED que já foi com sucesso combinada com a técnica original de ExM. Com a combinação destas duas técnicas será possivél obter resoluções já muito para além dos limites de difração, mas seria necessário o desenvolvimento de fluoróforos para coloração fluorescente baseados em nanocorpos ou moléculas pequenas que sejam compatíveis com a técnica de X10 ExM, devido à distorção na imagem que começa a ser criada pelo tamanho dos anticorpos convencionas utilizados ao chegar-se a resoluções muito elevadas. Após a combinação destas técnicas ficar viável poderia-se efetuar Z-stacks destas inclusões de ASYN heterogéneas com immunostaining feito também para outras proteínas que fazem parte da composição dos CL, potenciando desta forma uma análise muito mais detalhada da estrutura destas inclusões por estudos de co-localização. Para estudar estas inclusões num ambiente mais fisiológico ao qual os CL tendem a ser encontrados, estas técnicas poderiam ser aplicadas também a células de cultura primária de neurónios que possuem o fenótipo dopaminérgico, ou até a células imortalizadas que foram diferenciadas para obter esse fenótipo, algo que não está presente em células H4. Este fenótipo é escolhido devido à presença de CL na *substantia nigra pars compacta* do mesencéfelo em pacientes que possuem a DP.

O uso de técnicas de microscopia de super-resolução demonstra ser uma ferramenta extremamente importante para o estudo de sinucleinopatias, com técnicas como X10 ExM, mesmo necessitando de alguma optimização, sendo de extrema importância pela acessibilidade que traz à obtenção de resoluções de 25 nm que são comparáveis a outras técnicas topo-de-linha. A utilização desta técnica sozinha ou junta com outras de microscopia de super-resolução pode ser a chave para um entendimento melhor da composição, estrutura e função dos CL e poderá abrir a porta para o desenvolvimento de novas estratégias que ajudem a lidar com as sinucleinopatias.

Palavras-chave: alfa-sinucleína, Doença de Parkinson, microscopia de expansão X10, inclusões, STED

Abstract

Parkinson's Disease (PD) and Dementia with Lewy Bodies (DLB) are two of the most common neurodegenerative diseases that affect humans, which despite the vast amounts of studies that have been done trying to understand these diseases, there is still a lot left to uncover if we ever hope to find a way to combat these pathologies. Given that the alpha-synuclein-containing Lewy Bodies (LB) are a common main histopathological hallmark of these diseases, a better understanding of these abnormal aggregations, namely their composition, architecture and function, could lead us a step further in understanding how to prevent neurodegeneration from occurring due to these pathologies.

The main focus of this project relates to how super-resolution microscopy techniques (namely X10 Expansion microscopy (ExM) and Stimulated Emission Depletion (STED)) may be utilized in order to study alpha-synuclein (ASYN) inclusions that can be found in H4 cells transfected with a modified ASYN containing a C-terminal tag in the form of a truncated enhanced green fluorescent protein (SynT) and Bimolecular Fluorescence Complementation (BiFC) models, while also performing immunostainings for other proteins that have been found present in the structure of LBs. Of the two super-resolution microscopy techniques a higher focus on the X10 expansion microscopy technique, that allows for the achievement of resolutions around 10 times what you would usually accomplish without requiring a higher-end microscope. With this technique it was possible to observe large inclusions in the aforementioned transfection models that showcase an LB-like heterogenous structure, and also permitted a more detailed look at the free ASYN present in the cells' cytoplasm. The usage of X10 ExM, however, faces some drawbacks in terms of loss of fluorescent signal that can lead to some immunostained proteins being undetectable from fluorescence microscopy and with the general time that is required for the procedure. Despite these drawbacks X10 ExM still shows promise as a technique that could allow super-resolution microscopy reach a wider usage in comparison to its more expensive super-resolution microscopy counter-parts thanks to it being a relatively cheap and easy to access method. The usage of different display placements and STED microscopy on the other hand, continue to be viable tools for the study of these inclusions, which could even be combined in the future with the X10 ExM technique to allow for the analysis of LBs at an even greater detail than ever before.

All in all, super-resolution microscopy techniques, after some degree of optimization, may be the key required for achieving a better understanding of these LBs, something that could very well be essential in learning about their involvement in PD and DLB, and through that possibly helping with the development of novel strategies that could allow us to deal with these pathologies.

Keywords: alpha synuclein, Parkinson's Disease, X10 Expansion Microscopy, inclusions, STED

I carried out the studies presented in this dissertation as an ERASMUS+ student at the Outeiro Lab in the Department of Experimental Neurodegeneration at the University Medizin Göttingen in Göttingen, Germany. These studies were performed from 9/9/2019 to 24/6/2020 under the supervision of Tiago F. Outeiro, PhD.

Table of contents

Index of tables

Index of figures

List of abbreviations

AD – Alzheimer's Disease

ALP – Autophagy-lysosomal pathway

ASYN – Alpha-synuclein

BiFC – Bimolecular fluorescence complementation

DNA – Deoxyribonucleic acid

DLB – Dementia with Lewy Bodies

EGFP – Enhanced green fluorescent protein

ExM – Expansion microscopy

HD – Huntington's Disease

iExM – Iterative Expansion microscopy

LB – Lewy Body

MSA – Multiple System Atrophy

NAC – Non-Amyloid Component

PD – Parkinson's Disease

RNA – Ribonucleic acid

sph-1 – Synphilin-1

STED – Stimulated Emission Depletion

STORM – Stochastic Optical Reconstrution Microscopy

SynT - aSynuclein fused with a non-fluorescent GFP fragment

TOM20 – Mitochondrial import receptor subunit TOM20

TUJ1 – Neuron-specific class III beta-tubulin

UPS – Ubiquitin-proteasome system

VCa – Alpha-synuclein protein fused with a venus protein fragment at its C-terminal

VNa - Alpha-synuclein protein fused with a venus protein fragment at its N-terminal

VNs – Synphilin-1 protein fused with a venus protein fragment at its C-terminal

µg - microgram

µL - microliter

1. Introduction

1.1. Protein Misfolding diseases

Neurodegenerative diseases are one of the current greatest threats to human health, with conditions such as Parkinson´s disease (PD), Alzheimer´s disease (AD), Amyotrophic lateral sclerosis, Huntington's diseases (HD) among others becoming increasingly prevalent in our society due to the rise of the world´s elderly population [1]. These pathologies are able to cause memory and cognitive impairment, as well as deficits in an individual's motor skills and their ability to speak or even breathe, which has led the diseases to be target of several studies all around the globe [1].

A large part of the neurodegenerative diseases are also protein misfolding diseases where proteins may gain an alternate stable conformation and affect the organism in two different ways. One is by developing a toxic gain-of-function, which may be achieved from protein misfolding leading to the aggregation of the protein into toxic oligomers, fibrils, or inclusions [2]. Another way protein misfolding can affect the organism is by leading to a loss-of-function, having the protein being directed to the cell's degradation systems, or through the aggregation of the protein leading to its loss-of-function, or even possibly causing the loss-of-function in the other subcellular proteins that may be incorporated into its inclusions [2, 3]. In diseases like AD and PD their pathogenicity seem to involve the misfolding of the tau protein and the alpha-synuclein protein, respectively [2].

A cell possesses quality control mechanisms that can act against protein misfolding, maintaining a cell's proteostasis. Here a cell's chaperones play a very large role, being responsible for maintaining a protein´s native and functional conformation by helping the folding of polypeptides when they are being synthetized from RNA, assisting a misfolded protein in returning to its native conformation [1, 4]. When folding the proteins to their native conformation is no longer viable, the chaperones may also act by directing misfolded proteins to protein degradation systems such as the autophagic-lysosomal pathway (ALP) and the Ubiquitin-proteosome system (UPS) when achieving the native conformation is no longer a viable option [1, 4]. The UPS functions by using the ubiquitin-activating enzyme (E1), ubiquitin conjugating enzyme (E2) and ubiquitin protein ligase (E3) to mark the target protein for degradation with an ubiquitin polypeptide chain, directing it for the 26S proteasome where the protein is degraded into small peptides [5]. The ALP usually works on misfolded proteins through chaperone-mediated autophagy (usually in response to toxic compounds or oxidative stress) where the cytosolic chaperones heat-shock cognate 70 lead the proteins to lysosomes for degradation [6].

Unfortunately, as a person ages their cells' proteostasis systems become less efficient, increasing the propensity for proteins to misfold into a non-native but still somewhat thermodynamically stable conformation. This in turn can facilitate their propensity their aggregation, which leads to a higher susceptibility to stochastic, late-onset protein misfolding diseases [7]. Besides an individual´s age, these diseases have the less common occurrence of being caused by heritable mutations, such as the case with HD (caused by aggregation of the huntingtin protein), PD and AD. In the case of the latter two this can lead to an early-onset of the pathology [4].

1.1.1. Synucleinopathies

Synucleinopathies are diseases that are associated specifically with the misfolding of the protein alpha-synuclein (ASYN) in neuronal and non-neuronal cells in the brain. ASYN, being a major component of inclusions known as Lewy bodies (LBs), can be formed in various regions of the brain through accumulation and fibrillation of ASYN into β-sheet-rich structures in a nucleation-dependent

polymerization, with a phosphorylation at Ser-129 being the predominant post-translational modification observed in these ASYN [8, 9]. These LBs were first found and named after Friedrich Lewy, who discovered the presence of abnormal proteinaceous inclusions in the brains of patients of PD, and ever since have been found to be present in many other neurodegenerative diseases such as PD with dementia, dementia with LBs (DLB), multiple system atrophy (MSA), among others. Not much is yet known about the structure or function of the LBs but it has already been found to possess more than 90 different molecules, including synphilin-1, ubiquitin, tubulin, various heat-shock proteins, lipids, and the inner mitochondrial membrane protein TOM20 [3, 8, 10].

1.1.1.1. Parkinson's disease

PD is the second most common neurodegenerative disease (after AD) and the most common synucleinopathy, affecting about 2-3% of the population over 65 years of age [11], being, as mentioned before, caused by sporadic mutations for around 90% of the cases. This becomes increasingly more common as a person ages, with the rest being caused by heritable monogenetic mutations (familial cases of PD) that have been observed to occur through autosomal dominant genes and autosomal recessive genes [12]. Due to improvements in PD therapies, including pharmacological dopamine substitution and the introduction of deep brain stimulation, both the quality of life and the life expectancy of people carrying the disease have greatly increased, showing that the disease can be effectively managed. The increased life expectancy in turn is also the reason for the increasing prevalence of the disease, with the number of carriers being expected to double from 2005 to 2030 [11].

PD's pathology includes the intracellular aggregation of ASYN, and the loss of dopaminergic neurons in the midbrain's *substantia nigra*, which leads to a dopamine deficiency (neither of which being specific to PD) [11]. The loss of dopaminergic neurons is exclusive to the ventrolateral substantia nigra, starting even before the onset of motor symptoms, and becoming more widespread as the disease progresses. Meanwhile, the accumulation of ASYN occurs in the cytoplasm of neurons in many different brain regions, usually forming LBs. These aggregations are first found in cholinergic and monoaminergic brainstem neurons and in neurons of the olfactory system. As the disease progresses, they also become observable in limbic and neocortical brain regions [11]. The protein has also been found to be present in many different organelles, such as in mitochondria of brain regions such as striatum, substantia nigra, and cortex [13], mainly in the inner mitochondrial membrane, possessing an affinity to the lipid cardiolipin, which is mainly found there [14, 15].

The study of heritable forms of PD and large genome-wide association studies has led to many molecular pathways having been found to be related to PD. These include: ASYN proteostasis, mitochondrial function, oxidative stress, calcium homeostasis, axonal transport and neuroinflammation [11].

1.1.1.2. Alpha-synuclein

The ASYN protein was first found to be associated with PD in a study released in 1997, where it was observed to be a major component of LBs and also associated with familial forms of PD, with all diseases caused by its aggregation being dubbed "synucleinopathies" [8].

This protein's function is still not very well understood, being ascribed to unknown roles in processes such as in membrane biogenesis, vesicle trafficking, synaptic release, and plasticity, and also dopamine synthesis and transport. The monomer of ASYN consists of three main regions (Figure 1.1): the

amphipathic N-terminal domain, which is responsible for membrane binding, containing a repetitive highly conserved α-helical lipid-binding hexamer amino acid motif "KTKEGV"; the C-terminal domain, that is rich in proline, glutamic acid and aspartic acids, and thought to possess a chaperone function; and the non-amyloid component (NAC) which plays a key part in its self-assembly and aggregation [16]. Many studies have been able to confirm the toxicity of its oligomeric and fibrillary forms, being observed to cause cell death both *in vitro* and *in vivo* [8], with a study even suggesting that its oligomeric or protofibril form may be the main cause of the synucleinopathies' neuronal cell death, whilst the fibrillary form may act in a more cytoprotective role [17, 18].

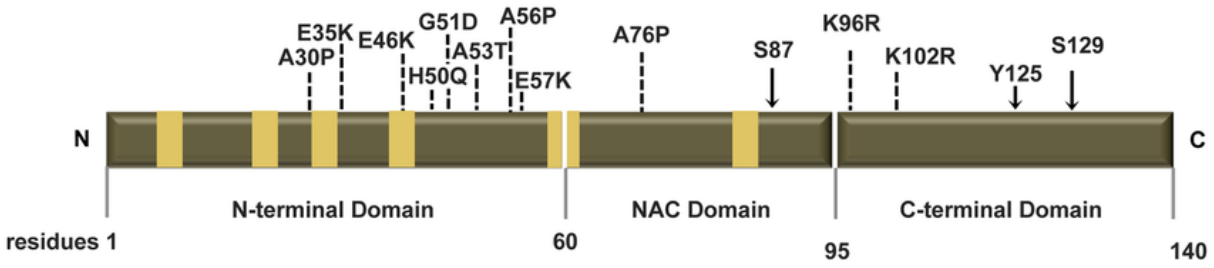

Figure 1.1 ASYN protein structure and its pathological modifications. The ASYN is a 140 residues-long protein that can be divided into its N-terminal Domain (responsible for membrane binding), Non-amyloid component (NAC) Domain (responsible for its self-assembly and aggregation), and C-terminal domain . Arrows showcase pathological post-translational modifications, while broken lines indicate known familial PD mutations. Yellow bars represent KTKEGV repeats; image adapted from [19].

The secondary structure of the ASYN can vary wildly, being natively unfolded whilst in aqueous solutions, and changing to an α-helical structure thanks to its "KTKEGV" motif once bound to lipid molecules or phospholipid membranes. It is also able to develop a β-sheet structure due to its NAC region's amyloidogenic properties, from its usual random coil conformation. The C-terminal region on the other tends to remain unfolded, in part due to its lack of interaction with other structures [16].

Studies have shown that while in physiological conditions the UPS seems to be the ASYN protein's primary degradation system, with its function being impaired in the presence of high levels of ASYN, and that the ALP system starts playing a role in ASYN degradation only after significant accumulations of the protein occur and cause stress for the cells, possibly in response to impairment of the UPS [20]. So, the UPS may act to degrade smaller aggregations of ASYN (oligomers) whilst the ALP deals with larger aggregates such as fibrillates or large oligomers [8].

ASYN aggregation also presents a significant impact on mitochondrial functions, having been shown to bind and accumulate to the mitochondria in ASYN over-expressing human neuroblastoma cells [21]. This causes oxidative stress by increasing formation of reactive oxidative species due to the cytotoxicity of the aggregates, increasing tyrosine nitration of several mitochondrial proteins, and decreasing the mitochondrial transmembrane potential, leading to a greatly impaired rate of cellular respiration, and leading to both cellular and mitochondrial malfunctioning [21].

1.1.1.2.1. SynT-Synphilin-1 transfection model

With the prevalent discussion on the role of LBs in the pathogenicity of PD, the need for models able to reproduce Lewy-like structures arises. One of the more prevalent models used has been the SynT transfection model (Figure 1.2), where co-transfection of the modified ASYN titled SynT with synphilin-1 (sph-1), a protein known to play a role in the formation of ASYN inclusions and that has been found to be present in the structure of LBs. This model has led to consistently good results in its ability to form Lewy-like ASYN inclusions. Here the SynT is an ASYN protein that contains a C-terminal tag in the form of an enhanced green fluorescent protein (EGFP) which has suffered a proteolytic cleaving (keeping amino acids 1-83) in which the EGFP loses its fluorescence, but nevertheless its presence is able to enhance the ASYN's propensity to aggregate. This cleaving of the EGFP previously occurred in vitro when the transfected ASYN contained the entirety of the EGFP protein [22, 23].

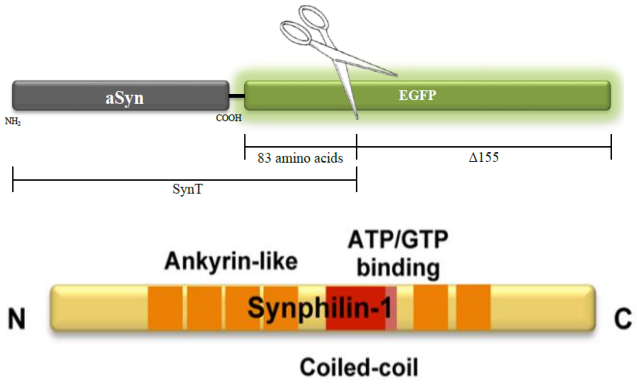

Figure 1.2 Depiction of the SynT and Synphilin-1 proteins involved in the ASYN aggregation model. The SynT is a protein composed of ASYN which is C-terminally tagged with an EGFP protein that's truncated, leaving only 83 amino acids and losing its fluorescence, and synphilin-1 is a ASYN interacting protein found to be present in Lewy Bodies; image adapted from [19].

Synphilin-1 is a neuronal protein first found through a yeast 2-hybrid assay that is enriched in presynaptic terminals, where it is found to interact with synaptic vesicles [24, 25]. This protein has also been determined to be part of the LBs structure, containing ankyrin repeats and a coiled-coil domain in its middle section, the latter of which has been found to interact with the N-terminal section of ASYN, from which it is able to facilitate the formation of ASYN inclusions [25].

The presence of the truncated EGFP in the protein's structure seems to somewhat maintain ASYN's natural conformation, but has been shown to lead to alterations in intermolecular and intramolecular interactions at the N-terminal section that have been found to regulate its aggregation, and also in the protein's membrane binding capabilities. These factors may be the cause for the protein's increased aggregation rate, instead of being the presence itself of EGFP causing it, all the while keeping the same rate of fibril formation as recombinant ASYN in similar conditions. Thanks to this model the visualization of ASYN aggregates through fluorescence microscopy has been greatly facilitated and allowing for a better study of the aggregates' effects on the cells and its subcellular distribution [23].

1.1.1.2.2. BiFC transfection model

Besides the LB ASYN inclusions, other structures that also possibly possess a large role in causing PD's pathology are ASYN oligomers, which have been found in many studies to be cytotoxic structures. Due to the difficulty in differentiating oligomers from ASYN monomers when visualizing cells through fluorescence microscopy, a transfection model named bimolecular fluorescence complementation (BiFC) has been used to overcome this problem [18, 22].

This model essentially involves the transfection of two proteins, each possessing a different section of a fluorescent protein, normally GFP or, more recently, the Venus protein (Figure 1.3). In the case with the transfection of two ASYN proteins, each is attached with a section of the venus protein at different terminal of the ASYN's structure due to the proteins' antiparallel interaction. These fluorescent protein fragments are non-fluorescent by themselves, only regaining that capability when different sections of the protein come together thanks to the oligomerization of two ASYN proteins. This interaction allows for a somewhat accurate visualization of the protein's oligomerization, facilitating the study of its subcellular distribution in a live cell. However, it is currently unknown how much the interaction of the GFP/Venus fragments may affect the oligomers stabilization, though comparison with other similar protein-protein interaction assays show that it is not causing the interactions themselves [18, 19, 22].

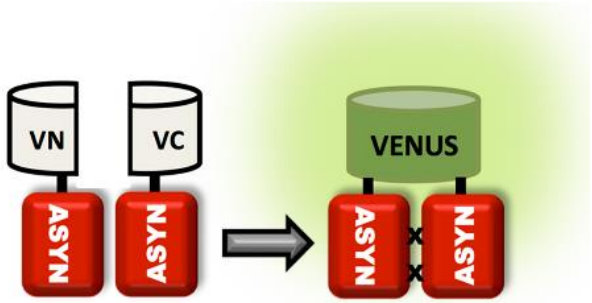

Figure 1.3 Venus protein-based BiFC model on ASYN. The image depicts the basis for the BiFC model, with 2 different ASYN proteins, each containing a section of the fluorescent Venus protein (named VN and VC after the terminal section of the ASYN protein that they're attached to), and showing the protein being reformed through the antiparallel interaction of the two ASYNs; image adapted from [19].

1.2. Super-resolution microscopy

As microscopy technologies evolved, one of the greater challenges it faced was the diffraction limit, which limited how much an image could be amplified until it was no longer possible to increase its resolution, ending up at a maximum possible resolution of 200-350 nm. To overcome this, several super-resolution microscopy techniques have been developed that allow to bypass the diffraction and obtain images of increasingly larger size without sacrificing image detail [26].

1.2.1. Stimulated emission depletion microscopy

Stimulated emission depletion (STED) microscopy, developed by Stefan W. Hell and Jan Wichmann in 1994, for which Hell received a Nobel Prize in Chemistry in 1994, super resolution technique that allows images to be taken at a higher resolution than the diffraction limit [27, 28]. STED differs from techniques such as Single-molecule localization microscopy and Structured illumination microscopy by working through the reduction of the size of the point spread function, and by not requiring software analysis after image acquisition [29, 30].

This technique essentially functions through the usage of two types of lasers, the first being the excitation laser that is used in conventional fluorescence microscopes, which causes fluorophores in a certain area to pass from their ground state to a singlet excited-state. The other laser utilized, which is specific to this technique, is a depletion laser (or STED beam) that is tuned in a wavelength that allows it to cause the passage of the fluorophores from excited-state to their ground state via stimulated emission, causing the de-exciting of fluorophores in a doughnut-shaped area. The effect of the STED beam then leaves only a 'zero'-intensity point in the middle to still possess fluorophores in their excited-state which are then still able to emit a fluorescent signal that can be detected by the microscope (Figure 1.4) [29, 30].

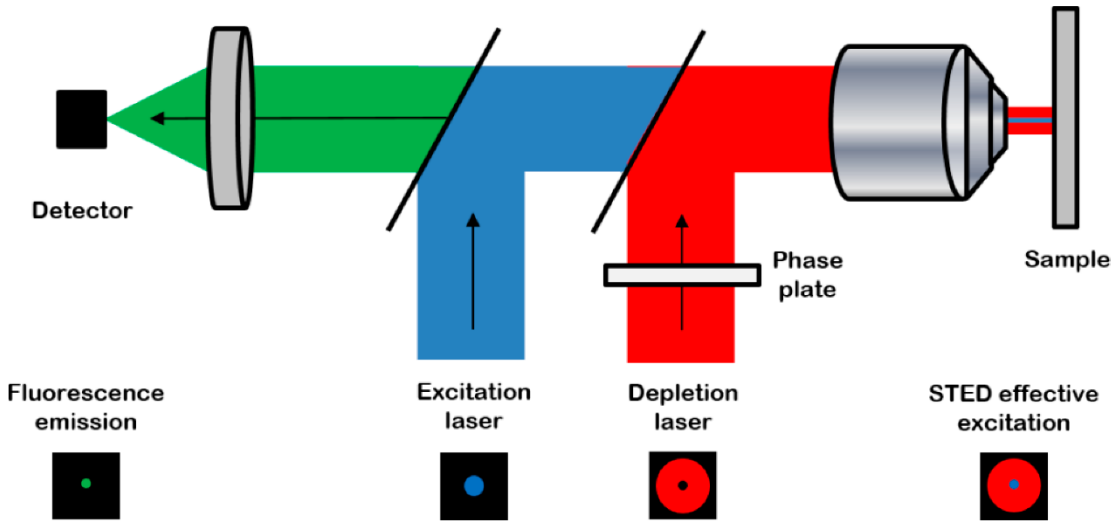

Figure 1.4 Schematic of a STED microscope. This technique utilizes a conventional excitation laser, and a depletion laser that can de-excite fluorophores in a doughnut shape around the excitation laser, leaving only a 'zero'-intensity point to emit fluorescence that can be detected by the microscope; image adapted from [31].

Through this process the technique allows the image resolution obtained to surpass the diffraction limit, by forming a 'zero'-intensity point of very reduced size, and allowing for a visualization of that area where its fluorophore(s) are more clearly differentiated from the ones surrounding the 'zero'-intensity point. This leads to the imaging of samples at a much higher quality than in conventional microscopes, reaching spatial resolutions of up to 20-30 nm, while having temporal resolutions of seconds, with the latter being comparable to a confocal microscope [26, 28, 29]. The usage of STED can even be theoretically able to obtain images in a molecule by molecule basis, reaching the highest possible resolution that could be obtained from fluorescence microscopy, but suffers from limitations caused by the signal-to-noise ratio [32].

1.2.2. Expansion microscopy

Expansion microscopy (ExM)) is a novel super-resolution microscopy technique that was developed with the intent of creating a technique that was not bound by the necessity of possessing either high-cost specialized equipped, and the usage of complex imaging analysis. And so, the greatest advantage of the technique is that it can be used regardless of the fluorescence microscope being used, since all the work is done on the samples themselves, rather of being in the way the images are obtained [26].

The technique was introduced by the Boyden laboratory in 2015 and it involves the physical magnification of the cells, which is done by attaching the samples to polyelectrolyte gels, followed by dialyzing them in water causing the expansion of the gel's polymer network, and in turn expanding the samples that the gel contains, whether they are cell cultures or even cell tissues [26, 33].

This first showcase of the technique allowed for expansion of samples to around 4x in each dimension, which is the equivalent of obtaining an image resolution of around 70 nm. Here the samples are fixed in a gel matrix that is composed of sodium acrylate, along with the cross-linker N-N'-methylenebisacrylamide and comonomer acrylamide, which then go through free radical polymerization through the usage of the catalyzers tetramethylethylenediamine (TEMED) and ammonium persulfate. Then the gel and the samples are digested through the usage of protease, homogenizing the samples to allow them to expand freely with the gel during expansion and preventing the appearance of distortions in the resulting images that could be caused from parts of the sample not getting separated and therefore not expanding properly. The final step in the procedure involves the repeated additions of excess volumes of water to the gel to cause its expansion, resulting in a 4 or 5-fold linear expansion (Figure 1.5) [33].

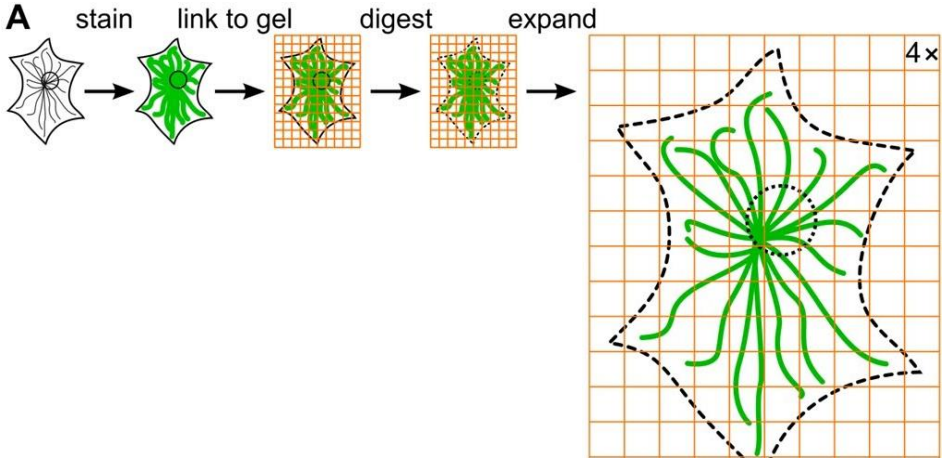

Figure 1.5 Visualization of the steps involved in ExM. The sample starts by being immunostained with fluorescent antibodies. It is then anchored to a gel matrix, from which it suffers digestion with a protease, and lastly is expanded along with the gel through the addition of excess volumes of water; image adapted from [34].

To properly observe the samples after an expansion procedure it was first required to perform a custom fluorescent labeling prior to the gelation step that would be able to endure the proteolytic digestion of the procedure. This involved the usage of a methacryloyl group which participates in the gel's polymerization, a fluorophore, and an oligonucleotide capable of hybridizing to a secondary antibody. This step was essential in the first published version of the procedure since there was no protein retention in the gel matrix, so the fluorophore's themselves had to be anchored to the gel, permitting the visualization of the proteins of interest [33]. A year later the same laboratory developed a slight variation on the procedure titled "protein retention expansion microscopy". The main difference from the previous version of the technique involved the usage of the anchoring reagent succinimidyl ester of 6-((acryloyl)amino)hexanoic acid (acryloyl-X SE), which is able to modify the amines on proteins with an acrylamide functional groups, anchoring them to the polymer network. Through the usage of this anchoring reagent, it was possible to use conventional fluorescent labelling techniques and also allowed the visualization of fluorescent proteins without necessitating their labelling [35]. One downside of the

ExM technique is that it requires the performance of fluorescence microscopy, due to how the high volumes of water mixed with the samples leading to them becoming increasingly more transparent [33].

The obtained resolution is a tremendous improvement over the previous microscopy techniques that are limited by the diffraction barrier, but unfortunately still falls short of resolutions that can obtained through high end super resolution microscopy techniques of modern stimulated STED and stochastic optical reconstruction microscopy (STORM) microscopes. To overcome this issue, two variations on the ExM technique have been developed to further increase its resolution [26, 33, 35].

1.2.2.1. Iterative Expansion Microscopy

Iterative expansion microscopy (iExM) was a technique first showcased in 2017 by the Boyden laboratory and allows a linear expansion of biological specimens of around 20×, allowing for resolution imaging of around 25 nm resolution in conventional microscopes [33].

This was possible through the application of two successive expansion procedures on the same sample, in which the first expansion is done with a polyacrylate gel matrix containing a crosslinker that is cleavable at high pH, such as N,N'-(1,2-dihydroxyethylene) bisacrylamide (DHEBA). Thanks to the usage of these crosslinkers after a first expansion the gels can be dissolved through the cleaving of their crosslinkers. This allows the samples to be added to a second polyacrylate gel, this time using the gel matrix composition of the conventional expansion procedure, which after another expansion procedure leaves us with an expansion factor of around 16-22× (4.5-5.5× in the first procedure, and around 4x in the second one), obtaining a resolution that is finally comparable to that of high-end super resolution microscopy techniques. Unfortunately, the resolution obtained ends up being capped at 25 nm, even though the expansion factor could in theory allow for greater resolutions, due to the distortions that start to be created from the size of conventional fluorophores being too large to be able to accurately portray some smaller cellular structures. This however can be resolved in the future through the application of nanobody-based or small molecule tags, although none have yet been made compatible to the iExM procedure [36].

1.2.2.2. X10 Expansion Microscopy

Since a normal expansion procedure can take almost a week to arrive at the point where the samples have been expanded, performing an iExM can end up costing a considerable amount of time. So, a new variant of the ExM technique was showcased in 2018 from the Rizzoli laboratory in Göttingen, titled X10 Expansion Microscopy (X10 ExM). The main difference this procedure has from the established ExM is the application of a gel matrix containing N,N-dimethylacrylamide acid (DMAA) with sodium acrylate, which then suffers free radical polymerization with potassium persulfate (KPS) and TEMED. This leads to a gelation reaction that occurs initially at extremely high speeds and that can be easily disturbed by the presence of oxygen, making it so the reactions have to be performed at low temperatures and with N_2 bubbling, and needs to be quickly applied to the samples, after which it requires a period of incubation of 6-24 hours for the complete polymerization reaction to occur [26]. Another difference that this procedure possesses in comparison to the normal ExM is that it requires a more severe digestion step, having the samples incubate with Proteinase K at 50ºC instead of room temperature. This is necessary since at a larger expansion factor it becomes more difficult to maintain sample integrity with a milder digestion step, although the increased digestion has the downside of impeding fluorescent proteins from being visualized without also going through fluorescent labelling [26, 37, 38].

These changes to the conventional ExM procedure result in an expansion factor of around 10×, that can even reach up to 11.5×, achieving an image quality that is equivalent to resolutions of 25-30 nm, which are comparable to those obtained from high-end super resolution microscopy techniques. Another great advantage is that the procedure and at a much lower cost, not requiring any expensive equipment in comparison to other super-resolution microscopy techniques, and only involving one expansion step, unlike iExM, making X10 ExM one of the better and most accessible super-resolution techniques [26].

2. Objectives

LBs are still very much an unknown variable in synucleinopathies, so in order to find out the role that LBs possess in pathologies such as PD and DLB it is necessary to have a better understanding of these inclusions' composition and structure, for which the usage of super-resolution microscopy techniques could prove essential. Thus, the main goals of this project were as follows:

a. Utilize the novel X10 Expansion Microscopy technique and STED microscopy in cells with ASYN inclusion forming SynT and BiFC transfection models and see what advantages the former may bring for the study of these inclusions.
b. Perform co-localization studies with other proteins known to be part of LBs and see if it is possible to obtain a better analysis of the structure of these inclusions with the usage of the X10 microscopy technique.

3. Materials and Methods

3.1. Production of Plasmid DNA

In this study plasmid DNA of SynT, synphilin-1-v5, pcDNA, and Venus protein containing the aSyn protein either at its C-terminal or its N-terminal (VCa and VNa, respectively), or containing a synphilin-1 protein at its N terminal (VNs), was produced in order to transfect cells with either the SynTtransfection model or a BiFC transfection model.

This was done by filling one 50 mL Falcon tube for each of the different plasmids, with 10 mL of LB medium, adding Ampicillin at a dilution of 1:1000 (10 µL in this case) in order to kill any bacteria that does not possess the plasmid gene, and then introducing bacteria containing the plasmids to each Falcon tube. This solution is then left mixing in a 37ºC incubator overnight, with 16 hours being necessary to obtain bacteria at the exponential phase of their growth.

Afterwards the contents of the Falcon tubes are added into a 1 L Erlenmeyer for bacterial growth, containing 250 mL of LB medium and 0.25 mL of Ampicillin. This solution is again left agitating overnight at 37ºC.

The extraction and purification of the plasmid DNA was performed according to the NucleoBond® Xtra Midi user manual, and later the concentration of DNA was measured utilizing the NanoDrop Spectrophotometer.

3.2. DNA electrophoresis in agarose gels

Following the purification of the plasmid DNA an electrophoresis procedure was performed in order to guarantee that the plasmids contained the expected DNA sequence. To achieve this 1 µg of each different type of plasmid is put into contact with 1 µL of green buffer (to allow the identification of the bands in electrophoresis through fluorescence), 7 µL of water and two specific fast digestion restriction enzymes at 0.5 µL each for 30 minutes at 37ºC in order to isolate the desired sequences from the plasmids. A similar mixture is done for each plasmid without the restriction enzymes and with 8 µL of water.

Afterwards the agar gel is formed utilizing 25 mL of 1.5% Agar with 5 µL of Ethidium Bromide (EtBr, which is used as a fluorescent tag), which after being formed has two lanes loaded for each different plasmid, one for the complete plasmids, and another for those cleaved with the restriction enzymes, and a lane with the marker GeneRuler™ 1kb DNA ladder. The gel is then left running at 100V for around 45 minutes.

3.3. Cell Culture

Human neuroglioma cells (H4) and were maintained in an OPTI-MEM® medium and Human embryonic kidney 293 cells (HEK) were maintained in an DMEM® medium. Both culture mediums were prepared with Fetal Bovine Serum (10%) and Penicillin/Streptomycin (1%). The cells are incubated at 37ºC in an atmosphere of 5% CO_2.

The cells are then plated with 70.000 cells/well in a 12-well plate and left to incubate for 24 hours before beginning the transfection.

3.4. Cell transfection

- SynT+synphilin-1

Before the transfection, FuGENE® HD transfection reagent (Promega) was added to Opti-MEM® serum-free and incubated for 5 minutes at room temperature.

The ratio between the mixture of Plasmid DNA and FuGENE® HD transfection reagent was 1:3. Plasmids encoding for SynT and synphilin-1 were added in equal amounts (1 µg each at a concentration of 1 µg/µL), after which the solution is incubate for 30 minutes. The solution was then added to the H4 cells and incubated for 48 hours.

- BiFC

The BiFC transfection model involved the transfection of a Venus protein containing either the aSyn protein or synphilin-1. For this project co-transfection was done of either VNa+VCa (for the study of ASYN oligomerization) or VNs+VCa (for the study of ASYN aggregation).

For this transfection 4µL of METAFECTENE® is added to 50µL of Opti-MEM® serum-free and is left incubating for 5 minutes. Simultaneously a solution is made mixing 50µL of Opti-MEM® serum-free with plasmid DNA being added of either VNa+VCa or VNs+VCa being added at equal amounts (1 µg each at a concentration of 1 µg/µL). The plasmid DNA solution is then added to the METAFECTENE® solution, and is then incubated for 20 minutes at room temperature before being added to the H4 cells

After adding the transfection solution, the cells are left incubating at 37ºC for 48 hours before they are further used.

3.5. Immunocytochemistry

After waiting 48 hours for the transfection to occur the wells are washed once with PBS, and then the cells are fixed with 4% PFA for 15 min, after which they are again washed with PBS for three different times. The cells are then permeabilized with 0.1% Triton X-100 (Sigma-Aldrich) for 20 minutes, followed by the blocking of the cells with 1.5% BSA/DPBS.

Subsequently several different primary antibodies may be added to the cells for 3-4 hours at room temperature or, alternatively, overnight at 4ºC. The primary antibodies (Table 3.1**)** which in the case of this project usually the usage of an ASYN antibody either alone or couple with the primary antibody which would mark a structure/protein that has been known to be affected by the presence of ASYN in the cell. This is followed by the washing of the cells with PBS 3 times and the addition of a secondary antibody (Table 3.2) for each primary antibody used before, now with an incubation time of 1-2 hours at room temperature. And finally, the cells are stained using DAPI (1/5000 in DPBS) to allow the visualization of the nucleus, followed by a final wash of the cells, which are then maintained with DPBS at 4ºC until their usage.

Primary antibodies:

Table 3.1 List of the different primary antibodies utilized for this study. Starting with the two antibodies utilized for ASYN and followed by the 6 targets chosen for the study of colocalization with ASYN: anti-ubiquitin, anti-Heat shock protein 70, anti-TIP47 for detection of perlipin-3, anti-TOM20 for mitochondrial detection, anti-TUJ1 for the detection of tubulin beta III, and anti-v5 tag for synphilin-1 detection.

Name	Species	Dillution	Solution	Reference	Company
anti-aSyn	mouse	1/1000	BSA 1.5%	610787	BD
anti-aSyn	rabbit	1/1000		ab138501	Abcam
anti-Ubiquitin	rabbit	1/400		ab7780	Abcam
anti-HSP70	mouse	1/200		ADI-SpA-810	Enzo
anti-TIP47	rabbit	1/250		NBP1-87871	Novus
anti-TOM20	mouse	1/500		sc-17764	Santa Cruz
anti-TUJ1	mouse	1/1000		MMS-435P-250	covance
anti v5-tag	mouse	1/200		46-0705	Invitrogen

Secondary antibodies:

Table 3.2 List of the different secondary antibodies utilized for this study.

Name	Species	Dillution	Company
Anti-mouse IgG Alexa-488	Donkey	1/1000	Invitrogen
Anti-rabbit IgG Alexa-488	Donkey	1/1000	
Anti-mouse IgG Alexa-555	Donkey	1/1000	
Anti-rabbit IgG Alexa-555	Donkey	1/1000	
Anti-rabbit IgG Alexa-633	Goat	1/1000	

3.6. X10 Expansion microscopy

To prepare the samples for expansion microscopy after their immunostaining they must go through a process lasting around 4 days and divided into 4 main steps: Anchoring treatment, gelation, digestion, and the expansion itself.

- Anchoring treatment

To allow the anchoring of the cells with the swellable gel formed in the next step, they are treated with a solution containing Acryloyl X-SE (Life technologies: A20770) in anhydrous DMSO at 0.1 mg/mL concentrations, which is stored desiccated at -20ºC. Acryloyl X-SE is then diluted 1:100 with PBS and then added as 80µL droplets for each 18mm coverslip inside a humidified chamber formed using a Petri dish containing wet tissues and covered in aluminum foil. The samples are then left at room temperature for at least 6 hours or even overnight, and at this point the samples can be stored at 4ºC in the dark for a long period of time.

- Gelation

For X10 expansion the gel matrix produced is composed of N-dimethylacrylamide acid (DMAA; Sigma-Aldrich: T7024) and sodium acrylate (SA; Sigma-Aldrich: 71289) at a molar ratio 4:1 (DMAA:SA) in ddH_2O. It is essential at this point to purge O_2 from the solution by bubbling it with N_2 gas for at least 40 minutes since it would inhibit the monomers' polymerization reaction. Afterwards a solution of

Potassium Persulfate (KPS; Sigma-Aldrich: 379824) of 0.036 g/mL is mixed with the monomer solution at a ratio of 10:1, which then needs to be bubbled with N_2 again for 15 minutes, which needs to occur with the solution surrounded by ice with water in order to avoid the gelation from occurring too soon.

Finally, for each two 18mm coverslips a solution is created by mixing 170µL of the gelation solution made, with 0.68µL of N,N,N',N'-tetramethylethane-1,2-diamine (TEMED; Sigma-Aldrich: T7024), which is then added to the coverslips in 80µL droplets in another humidified chamber (after washing each coverslip twice with DPBS beforehand). The gel is then left to incubate overnight at room temperature.

- Digestion

For the digestion of the samples a digestion buffer must be made consisting of: 50 mM Tris(hydroxymethyl)-aminomethane (TRIS; AppliChem: A3452), 1mM EDTA (Sigma-Aldrich: EDS), 0.5% (vol/vol) Triton X-100 (Sigma-Aldrich: 93426), and 0.8M Guanidine HCl (Sigma-Aldrich: G4505) in ddH_2O. After adjusting the solution to achieve a pH of 8.0 it can be stored as aliquots at -20ºC, and right before using it Proteinase K (Sigma-Aldrich: P4850) must be added at a ratio of 1:100 (reaching a final concentration of 8 units/mL).

The solution is added to the coverslips in a 12-well plate with 1mL of digestion buffer per well (for 18mm coverslips), the plate is then covered in a wet tissue and aluminum foil to decrease evaporation and is then incubated overnight at 50ºC.

- Expansion

In order to expand the samples each of the coverslips must be added into a different petri dish that is at least ten times its size, which are then filled with excess volumes of ddH_2O around 5-6 times (depending on how fast the gel increases its size by ten times) for 20-30 minutes. The expansion factor was measured by putting a square sheet paper beneath the petri dish containing the gel and measure the amount of squares taking up the diameter of the gel, and then dividing it by the diameter of the of the coverslip used.

After this the samples are finally ready for imaging, where portions of the gel are removed and put into a 60mm petri dish.

3.7. Fluorescence microscopy

- **Leica microscope**

In order to compare the effect of expansion on the cells' images were taken of them before and after the expansion procedure utilizing the 10×, 20×, and 40× objective with a Leica epifluorescence microscope (Leica DMI 6000B microscope), with the 63× objective being used only for pre-expansion samples, due to the difficulty that the lack of brightness in expanded cells imposes on the imaging of the cells. Here we mainly used the Alexa Fluor 488 on the ASYN protein when using more than one primary antibody, in order to be able to differentiate between BiFC's green fluorescent signal and the other proteins, and used Alexa Fluor 555 on ASYN when just imaging for that protein.

- **Olympus microscope**

An Olympus IX81-ZDC microscope system was utilized to observe H4 cells transfected with both used SynT models that were immunostained for ASYN and sph-1, before utilizing these cells for STED microscopy imaging, in order to confirm that the transfection and immunostaining was successful. Here the excitation beam ‘’650 CY5’’ was used for the ASYN proteins, stained with the goat Anti-rabbit IgG Alexa-633 secondary antibody and the excitation beam denominated ‘’470 GFP’’ for the synphilin-1 proteins that were stained with the donkey anti-mouse IgG Alexa-488 secondary antibody. These antibodies were chosen due to needing a large differentiation in signal wavelength to avoid signal overlap during STED microscopy.

3.8. Super-Resolution STED microscopy

Super-resolution STED microscopy was performed with a IX83 microscope (Olympus) based multicolor microscope setup (Abberior Instruments) that is equipped with an UPLSAPO 100x 1.4 NA oil immersion objective (Olympus). Here, as was previously mentioned, the microscope was used for the observance of ASYN and sph-1, with a 640 nm excitation laser being used for confocal ASYN imaging, and a STED 775 nm beam being used for STED ASYN imaging. And for sph-1 a 518 nm excitation laser was used for confocal imaging, with a STED 595 beam being used for STED imaging. Nearly all images were taken at a display orientation of XY with a range of 50 µm by 50 µm, and a pixel size of 50 nm by 50 nm.

3.9. Protein measurement

In order to measure the protein concentration of cells through the Bradford protein assay and prepare them for a western blot the cells must first be put on ice with RIPA lysis buffer (Abcam) for 5 minutes in order to cause cell lysis. After removing the cells from the well surface these must then be added into Eppendorf’s, which after 30 minutes on ice is put through cool centrifuging for 10 minutes at 14000 RPM, from which we remove the protein-containing supernatant.

With the proteins being extracted we can then add them, along with various concentrations of the standard curve protein (BSA), into a Bradford plate, with each sample and BSA concentrations added to three spots on the same line, mixing for each BSA well 50 µL of BSA with 150 µL of Bradford reagent (Bio-RAD), while 1 µL of the samples is mixed with 49 µL of H_2O and 150 µL of Bradford reagent. The protein concentration is then measured through the Tecan i-control™ software, which can directly measure the protein concentration of each well of the Bradford plate and even give an average for each sample.

3.10. Western blot

The western blots were performed by making a 12% Polyacrylamide separating gel, which was added into a cast with a 1.5 mm thickness and covered with isopropanol for 15 minutes, after which the isopropanol is removed and we add a 7.5% polyacrylamide stacking gel to the cast, immediately followed by the addition of the gel comb, and when the gel. Afterwards, 10 µg of protein is obtained from each cell lysate, mixed with the Loading dye, and heated for 5 minutes at 95ºC. Then, with the gel already in the running buffer, each sample is inserted into its own gel lane, and into a separate lane of the gel the PageRuler™ Plus Prestained Protein Ladder (10 to 250 kDa) (Thermo Fisher) is added. Following that an SDS-polyacrylamide gel electrophoresis (SDS-PAGE) is performed by leaving the gel running at 80V for 15 minutes and later at 110V for 1-2 hours.

When the SDS-PAGE is complete the gel is left in 20% Ethanol for 5-10 minutes, after which we utilize the iBlot™ 2 Gel Transfer Device (Thermo Fisher) to transfer the proteins into a nitrocellulose membrane. After checking that the proteins are present in the membrane with Ponceau S (Sigma-Aldrich) the proteins are blocked using BSA 5% in PBS-Tween shaking for 1 hour at room temperature. Afterwards the primary antibody, diluted in BSA 5%, is added to the membrane and left shaking overnight at 4ºC (or 3-4 hours at room temperature), followed by cleaning the membrane 3 times with TBS-Tween for ten minutes each, and finally the membrane is incubated with a secondary antibody diluted at 1:10000 in BSA 5% for 2 hours at room temperature.

Finally, the membrane is prepared for detection through the usage of enzyme linked chemiluminescence (ECL) detection reagents: Peroxide Solution and Luminol Reagent (Millipore) which are added at a 1:1 ration, after which the membrane's chemiluminescence can be observed through the western blot imaging system FUSION FX. After repeating these last steps from the addition of a primary antibody for the detection of β-actin it becomes possible to quantify the amount of protein in the membrane utilizing the image processing program ImageJ.

3.11 Measurement of the transfection rate

The measurement of the transfection rate was made from immunostaining and imaging two sets of H4 cells, taking at least 10 images of each different transfection of each set and calculating the ratio between transfected cells and the total number of cells in each image, measuring the average between the images, and then measuring the average between the two sets of cells.

4. Results

4.1. Choosing the transfection method to use on the SynT transfection model

In order to decide which transfection method would be better for the study of the SynT model an immunoblot and ICC was performed utilizing either the FuGENE® HD Transfection Reagent (Promega) or the Calcium Phosphate (CaPO) transfection method in H4 cells co-transfected with either SynT and pcDNA or SynT and synphilin-1. Results were also obtained for the METAFECTENE® transfection method in the interest of confirming that it can be used for cells transfected with the previously mentioned BiFC transfection models (VNaSyn+VCaSyn or VNsph+VCaSyn) (Figure 4.1 and 4.2), with the latter a novel model established in the Department of Experimental Neurodegeneration in Göttingen which allows for the study of ASYN inclusions and also the interaction between ASYN and sph-1. These transfection models are the only ones to be utilized for the entirety of the project.

The results obtained from the immunoblot went according to what was expected in terms of the molecular weight of each band and also in the significant difference of intensity between the VNa and VCa proteins [19, 39], with the sph-1 and VNa proteins' bands only appearing in cells that were transfected with those proteins, and the ASYN and VCa bands appearing throughout all the lanes. Already from a glance it is possible to notice that between the proteins transfected with FuGENE® and the ones transfected with CaPO, that the former possesses bands of higher intensity, something that was then confirmed through quantification analysis in ImageJ. This conclusion was also supported by the results that were obtained from fluorescence microscopy, with FuGENE® seemingly leading to a higher transfection rate in comparison to cells transfected using CaPO, leading to only the FuGENE® transfection method being utilized for the SynT transfection model from this point forward. The transfection rate for the BiFC cells is lower in comparison to the other transfections due to only the cells transfected with both proteins giving off a green fluorescent signal, but taking into account the results obtained from the immunoblot it seems that the usage of METAFECTENE® is adequate for the transfection of the BiFC model.

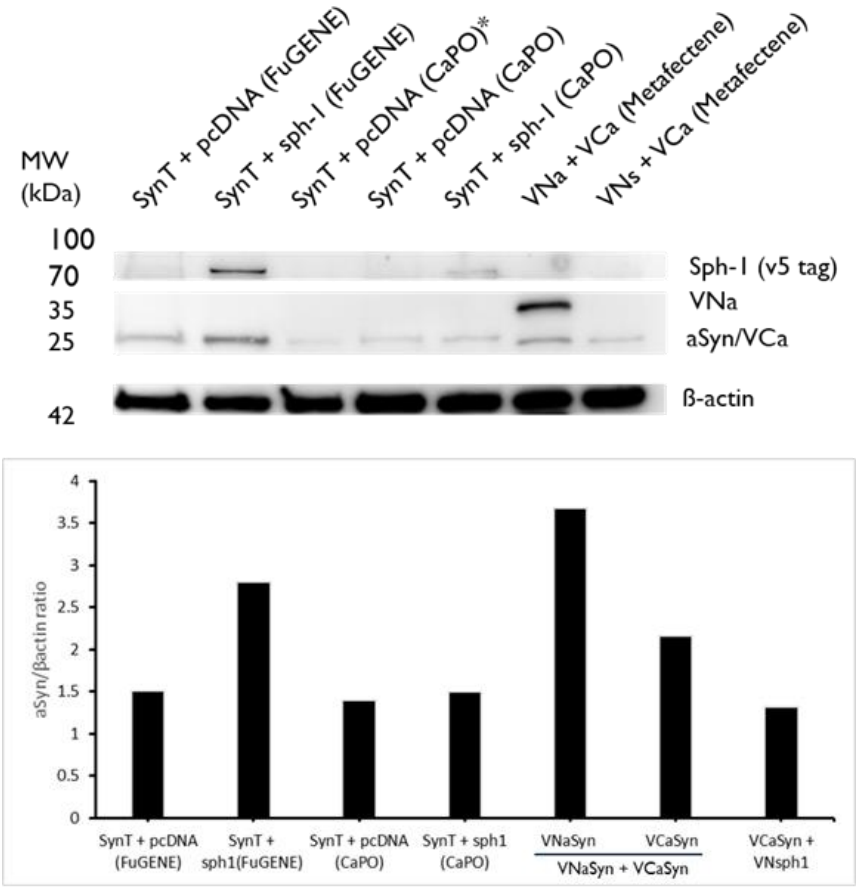

Figure 4.1 Immunoblot analysis of the level of expression of ASYN and sph-1 with different transfection methods and transfection models used. Immunoblot of ASYN and sph-1 confirming these proteins have been successfully transfect, showing SynT and v5-tagged sph-1 after transfection with both FuGENE® and CaPO methods, and VNa/VCa transfected with METAFECTENE® reagent, with β-actin used as loading control. There exist 2 lanes for SynT+pcDNA transfected with CaPO, with only the second lane being used for quantification analysis. Quantification was then analysed through the ratio of the intensity of the ASYN bands with the intensity of the β-actin bands, measured using ImageJ, showcasing a higher transfection level for the SynT transfection models transfected with the FuGENE® method. The high value of the ASYN/β-actin ratio, in comparison to what was to be expected due to the immunoblot images, occurred due to the image for the β-actin bands being at a lower resolution than the other ones, leading to a smaller image.

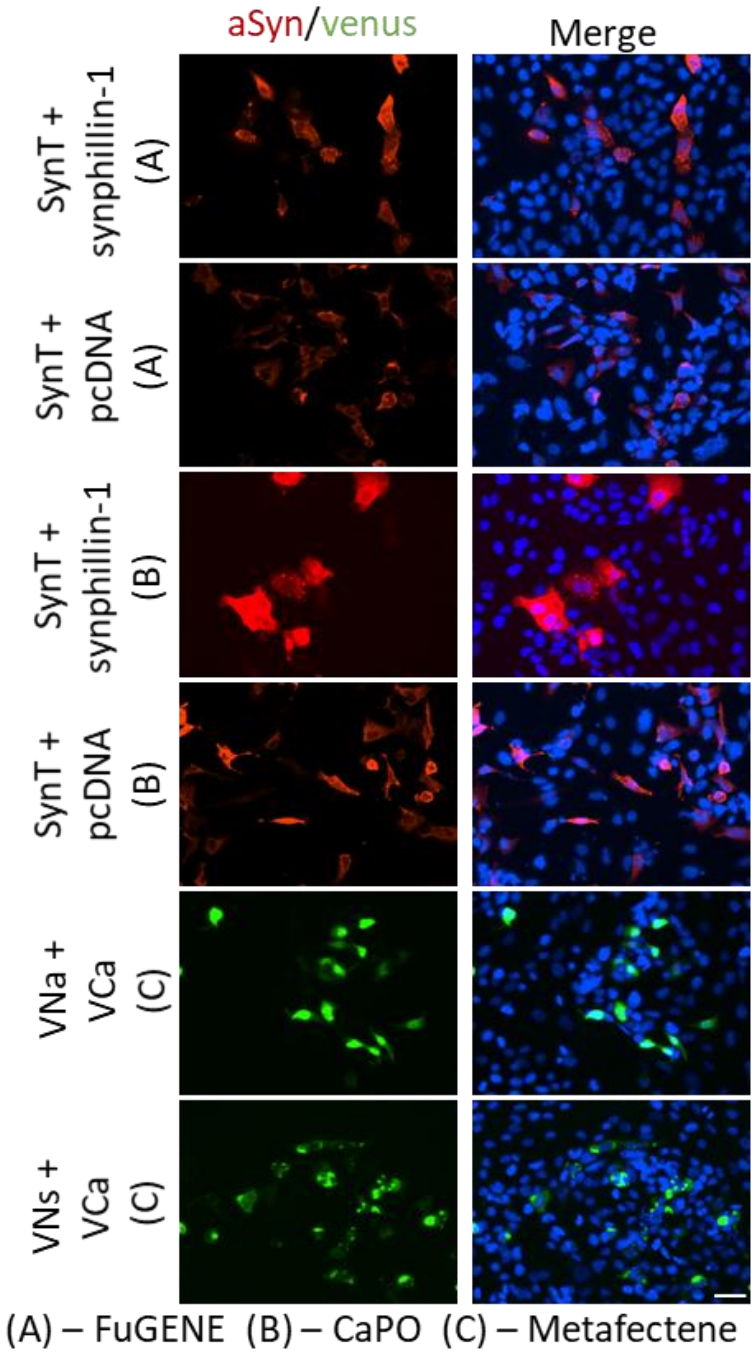

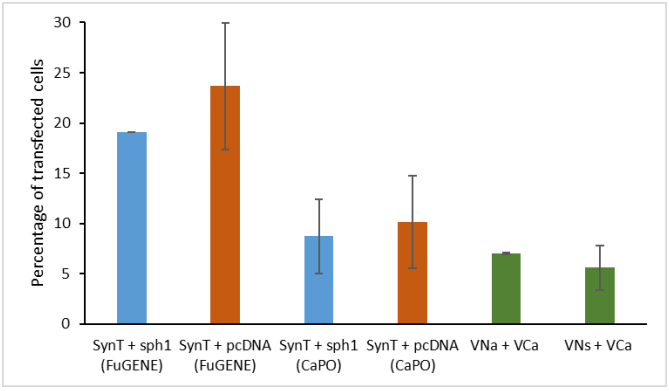

Figure 4.2 Immunocytochemistry analysis of the transfection level of ASYN using various transfection methods and the SynT and BiFC transfection models. ASYN – red; Venus protein – green; DAPI – blue. Through fluorescence microscopy of two different series of H4 cells it was possible to confirm that the SynT and BiFC transfection models produce the expected results, with the sph-1-containing H4 cells showcasing inclusions, and with the BiFC models giving of a fluorescent signal from the venus proteins. Scale bar is 50µm. By measuring the percentage of cells containing the transfected ASYN proteins in each image taken it was possible to measure the level of transfection from each different method and transfection model used, showing a higher percentage of transfection for the FuGENE® method.

According to the results obtained (Figures 6-7), the METAFECTENE® transfection reagent seems to be adequate for use in the BiFC transfection models, and FuGENE® HD seems to lead to a better transfection of the SynT transfection models in comparison with the CaPO transfection method.

In addition to the matter of the transfection method, these images also serve as confirmation that the transfection models are working as expected, with the BiFC models transmitting a green fluorescent signal and with inclusions being observed in the VNs+VCa and the SynT+Synphilin-1 models.

4.2. X10 Expansion microscopy on cells with SynT and BiFC transfection models

The first X10 Expansion microscopy procedure attempt was done on H4 cells that were transfected with the same models used before. These models are used to assess whether or not the ASYN would be observable after utilizing this microscopy technique. Imaging of the cells was done through fluorescence microscopy, obtaining images from before and after applying the X10 Expansion microscopy procedure on the cells (Figure 4.3), in order to better compare the differences observed from utilizing this super-microscopy procedure. It should be noted that due to the size of the gel obtained after the expansion of the cells, that obtaining images of the same cells before and after suffering expansion are not feasibly obtained.

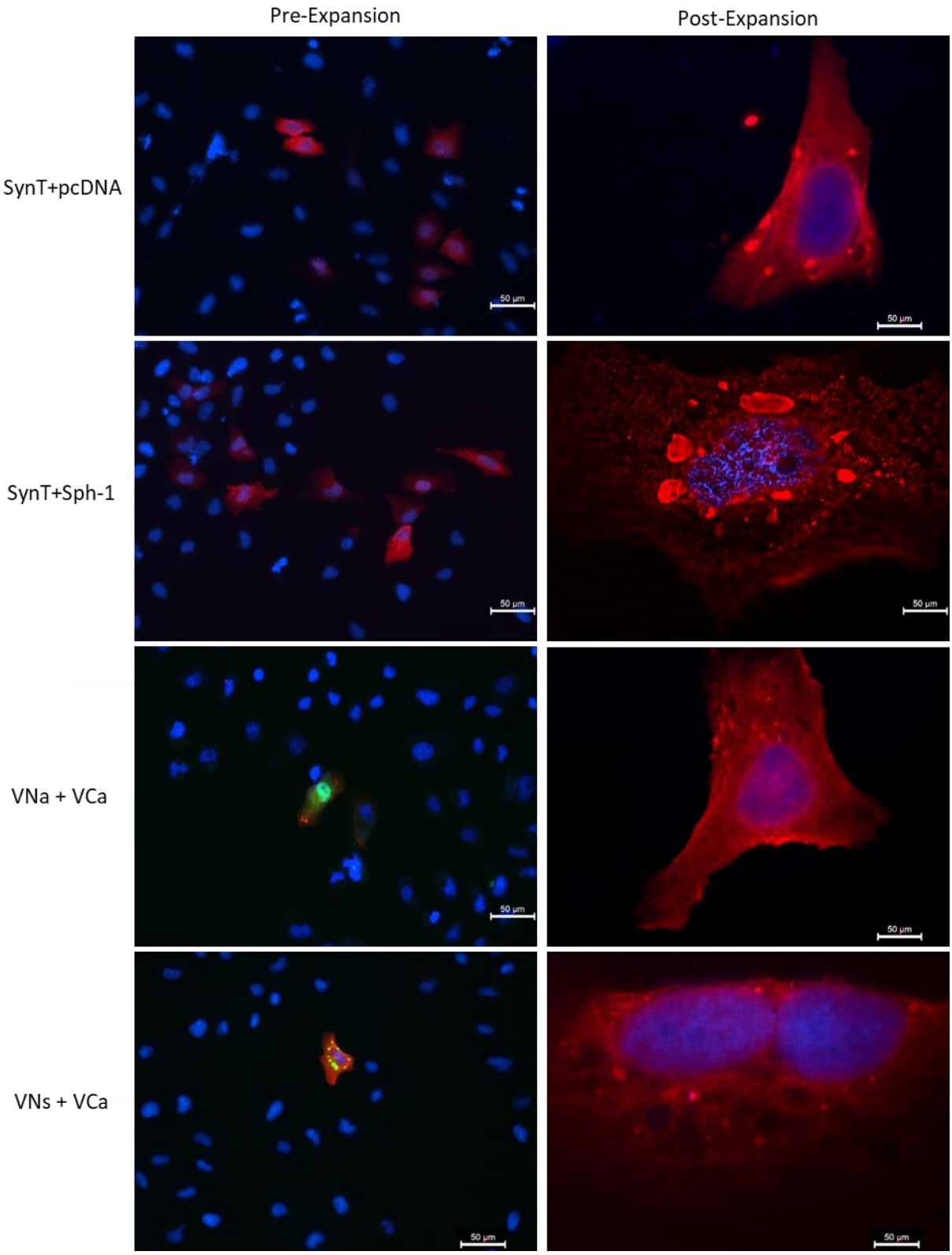

Figure 4.3 Comparison of H4 cells transfected with SynT and BiFC models before and after the X10 Expansion procedure at a 20x objective. The cells suffered an average expansion factor of 9.7x, allowing for a much better visualization of their contents, with the SynT transfection models proteins showcasing what seem to be large inclusions with an heterogenous structure. The BiFC transfection models seemingly lost their venus protein fluorescent signal, or at least had it lowered to a level that is not observable through this Leica microscope.

From the results obtained (Figure 8) it can be concluded that it was still possible to detect the ASYN protein, its inclusions, and the DAPI staining after the X10 expansion microscopy procedure. The

images obtained from post-expansion cells present ASYN throughout the cell as being distributed in a much more punctuated form, in comparison to the more diffuse background that is observed from images pre-expansion of the cells. This especially noticeable in the VNa+VCa cells which might be due to the transfection of two different variants of ASYN and the lack of formation of inclusions leaving more of the protein to be free in the cytoplasm. Meanwhile, the other transfected cells all showcase inclusions which, especially in the case of the cells transfected with the SynT model, appear to possess an heterogenous structure, which could make these inclusions somewhat closer in structure to a LB due to them also possessing an heterogenous structures, which comprises of over 90 different molecules [10]. This discovery shaped a lot of the work done afterwards for this project, which involves the study of the co-localization of ASYN with several other subcellular proteins that have already been found to be part of the structure of LBs. These studies would involve utilizing cells that go through the same four transfections utilized so far, in order to further see how these transfection models may allow for the imaging of LB-like inclusions and what the X10 Expansion microscopy procedure may bring for the imaging of such inclusions.

The venus protein's fluorescent signal, however, has either been severely reduced or completely depleted, most likely due to the digestion step of the expansion procedure that puts the cells into contact with Proteinase K, which could be putting a heavy strain on the interaction between the two different parts of the venus protein.

4.3. ASYN co-localization studies with and without X10 Expansion microscopy

In order to discover which subcellular components could be composing these heterogenous ASYN inclusions that were observed, it was decided to perform the immunostaining of subcellular components that were found to interact with ASYN. The ones chosen for this project were: synphilin-1, the microtubule component β-tubulin III, the mitochondrial import receptor subunit TOM20, ubiquitin, Mannose-6-phosphate receptor binding protein 1 (Perlipin-3) and the heat shock protein 70 (HSP70), all of these being proteins that have been found to be part of the structures of LBs [3, 10].

4.3.1. Decreased fluorescence of TOM20 and β-tubulin III after X10 ExM procedure precludes their detection

The microtubule component β-tubulin III and the mitochondrial import receptor subunit TOM20's presence in the ASYN's inclusions was the first to be attempted. In the case of TOM20 it was chosen due to the ability of some post-translationally modified versions of ASYN that allows it to form a high-affinity binding to the TOM20 protein, which is thought to be the cause of the mitochondrial dysfunction that leads to PD's pathogenesis [40], and in the case of β-tubulin III it was chosen due to its ability to co-localize with ASYN in the brains of MSA patients and also mouse models of MSA, leading to the neuronal accumulation of ASYN into inclusions [41].

The results obtained (Figure 9) from this study were unsuccessful due to the inability to detect these proteins after the expansion procedure. The lack of notable fluorescent signal from these proteins is probably due to the general lower signal intensity produced by the antibodies caused by the X10 ExM procedure, since it was possible to observe the proteins in images obtained of the cells before the expansion was performed. This problem would unfortunately persist throughout the rest of the project

with failed attempts being made to rectify this issue by increasing the concentration of antibody from the dilutions that were recommended in literature.

One thing to note from the obtained images of post-expansion cells (Figure 4.4) is that in the cells immunostained with TUJ1, the image from the sample of the cells transfected with the novel VNs clearly showcasing the presence of large heterogenous ASYN inclusions, showcasing how this model can be used alongside the SynT model for the study of LB-like inclusions in h4 cells.

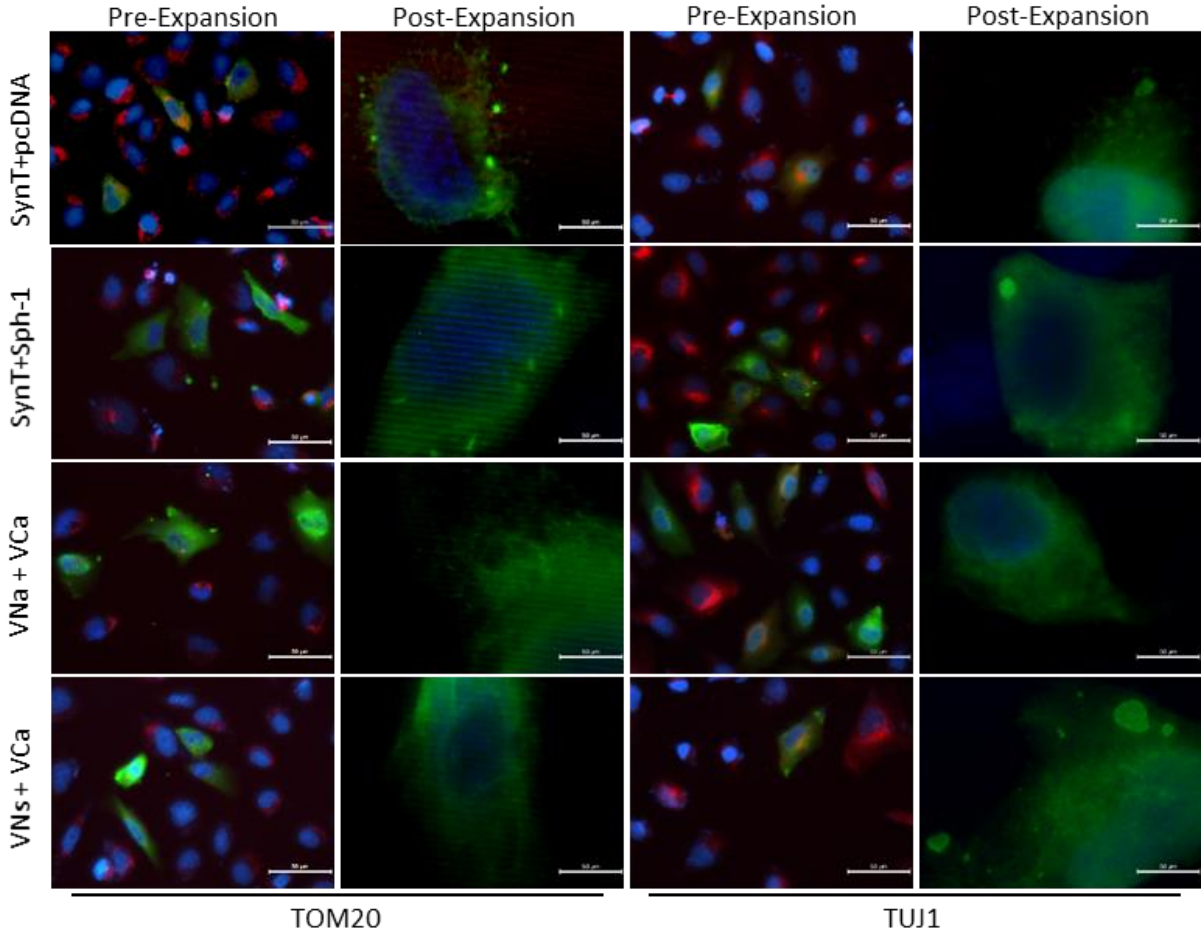

Figure 4.4 Comparison of pre- and post-expansion H4 cells stained for ASYN and either TOM20 or beta-Tubulin III. The images obtained show that the expansion procedure seems to a significant fluorescence loss for the TOM20 (left panels) and β-tubulin III (right panels) proteins (red), which difficulted the study of these protein's co-localization with ASYN (green)

From this point on, the focus shifted for co-localization studies on the images that were obtained of cells that have not gone through the X10 Expansion microscopy procedure, in order to showcase the value that these proteins would have for further study of heterogenous ASYN inclusions through Expansion microscopy and other forms of super-resolution microscopy. In the case of these two proteins, the samples with the TOM20 antibody did not seem to showcase co-localization with ASYN, although further study on this would be required since the protein was already found to co-localize with ASYN inclusions [40]. On the other hand, the TUJ1 antibody-containing cells seem to possess co-localization

of ASYN with the β-tubulin III protein in sph-1-transfected cells, showing how parts of the cytoskeleton may be recruited into the inclusions (Figure 4.5).

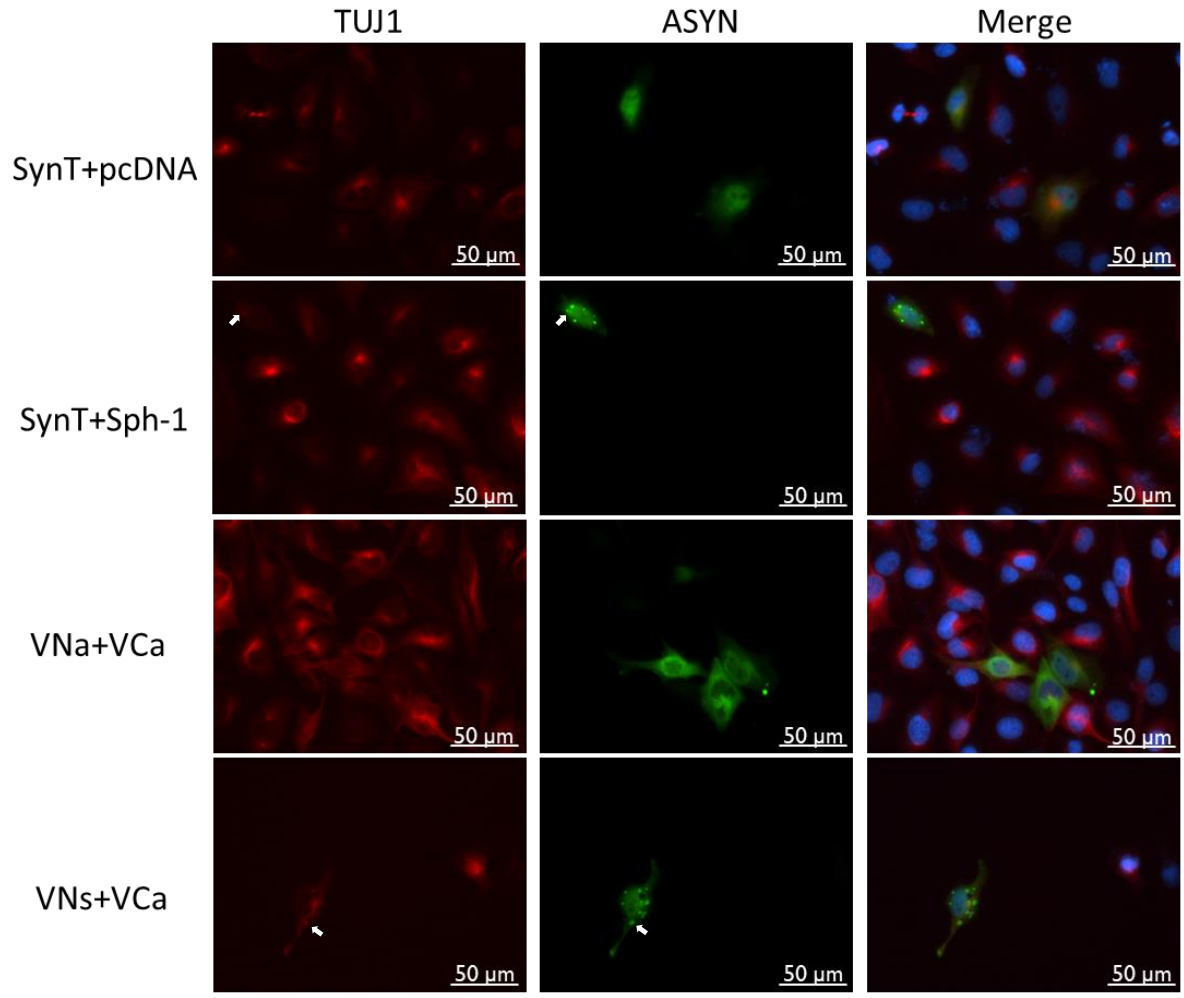

Figure 4.5 Co-localization of ASYN with TUJ1 without applying the X10 expansion procedure. From the immunostaining of ASYN and TUJ1 in H4 cells transfected with the SynT and BiFC models, co-localization of both in inclusions can be observed in the sph-1-containing models (SynT+Sph-1, VNs+VCa).

4.3.2. Synphilin-1 co-localizes with ASYN inclusions in the SynT model with transfected synphilin-1

Synphilin-1, as a protein that has been intensely studied over its involvement with the formation of ASYN inclusions, having been found as part of the structure of Lewy bodies, was a prime candidate for the study of ASYN co-localized proteins [24, 25].

Unfortunately, due to an unknown issue during the X10 expansion procedure of the cells with antibodies for sph-1 and the other following proteins, the gelation did not produce adequate results for a portion of the samples, which led to the inability to obtain images of some of the cell transfection models of each of the following immunostainings. Although the gels that were successfully formed were devoid of noticeable fluorescent signal outside of the one associated with ASYN or DAPI, similar to what had occurred for the TOM20 and TUJ1 immunostainings.

Through the images obtained of the cells before going through the X10 expansion procedure (Figure 4.6) it was possible to observe definite co-localization of ASYN with synphilin-1 in the SynT+sph-1 transfection model, which was to be expected given how its presence seems to facilitate the formation of the inclusions [24, 25].

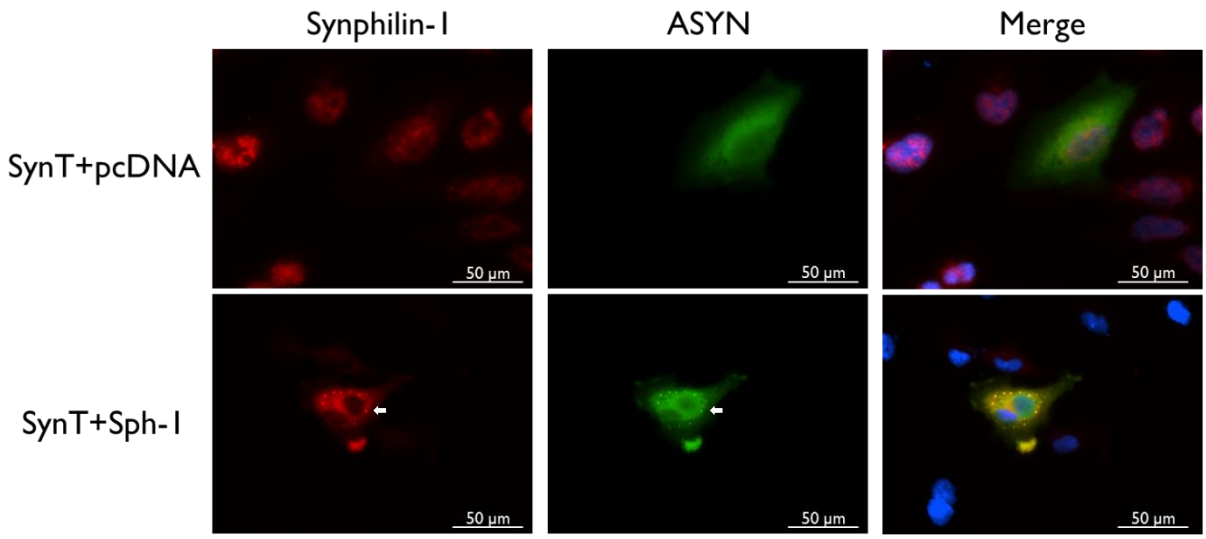

Figure 6 Co-localization of ASYN with sph-1. From the immunostaining of ASYN and sph-1 in H4 cells transfected with the SynT models. These images showcase co-localization of ASYN with sph-1 in cells transfected with both SynT and sph-1, whilst the other model still seems to be detecting sph-1, which may be a sign of low specificity of the v5-tag antibody.

4.3.3. Perilipin-3 co-localizes with ASYN inclusions in SynT and BiFC models

Perilipin-3 (also known as Mannose-6-phosphate receptor binding protein 1 or TIP47)) is a protein that is responsible for the regulation of lipid metabolism in lipid droplets, serving also as a marker for these vesicles. This protein was chosen due to having been found to interact with ASYN in several studies, possibly playing a role in changing the ASYN's conformation in an aggregation-prone form [42, 43].

The perilipin-3 protein was found co-localized with ASYN at the VNs+VCa and SynT+pcDNA transfection models (Figure 4.7). However, the absence of co-localization in the SynT+sph1 model occurred due to the failure of encountering inclusions in the observed cells, making the results of that

model inconclusive for this protein, although it would be expectable to also find co-localization in this transfection model.

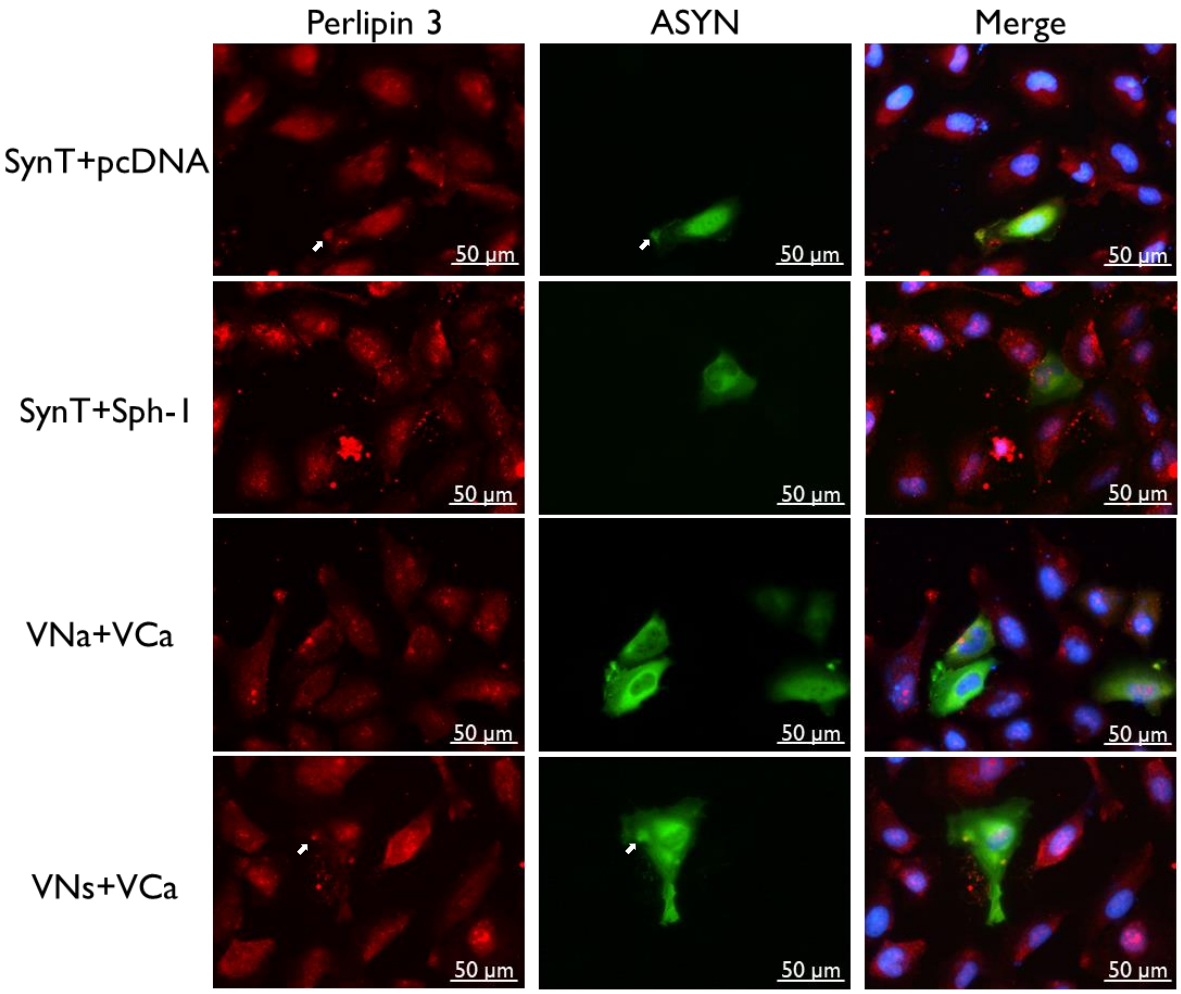

Figure 4.77 Co-localization of ASYN with Perlipin-3. From the immunostaining of ASYN and Perlipin-3 in H4 cells transfected with the SynT and BiFC models, co-localization seemed to occur in ASYN inclusions present in the VNs+VCa and SynT+pcDNA models. Lack of inclusions found in the SynT+sph-1 transfected cells due to an unknown issue.

4.3.4. Heat shock protein 70 co-localizes with ASYN inclusions in all inclusion forming models

The Heat shock protein 70 (HSP70) is a family of proteins that are expressed in response of stress in the cell, being able to form complexes with other chaperones allowing it to interact with peptide segments of misfolded proteins and either refolds them or leads the proteins to degradation in either the lysosome or the proteasome. Due to this the protein is instrumental in preventing neurodegeneration, having been found to be able to prevent the formation of ASYN oligomers and inclusions, and the failure to act successfully on these aggregations is what probably leads the protein to be observable in some LBs, making it a good target for this study [44, 45].

The images obtained without having applied the X10 expansion procedure (Figure 4.8) showcase clear co-localization of this protein with ASYN in the SynT+pcDNA, SynT+sph1, and VNs+VCa models, being the only of the studied proteins to showcase this in three of the four transfection models utilized.

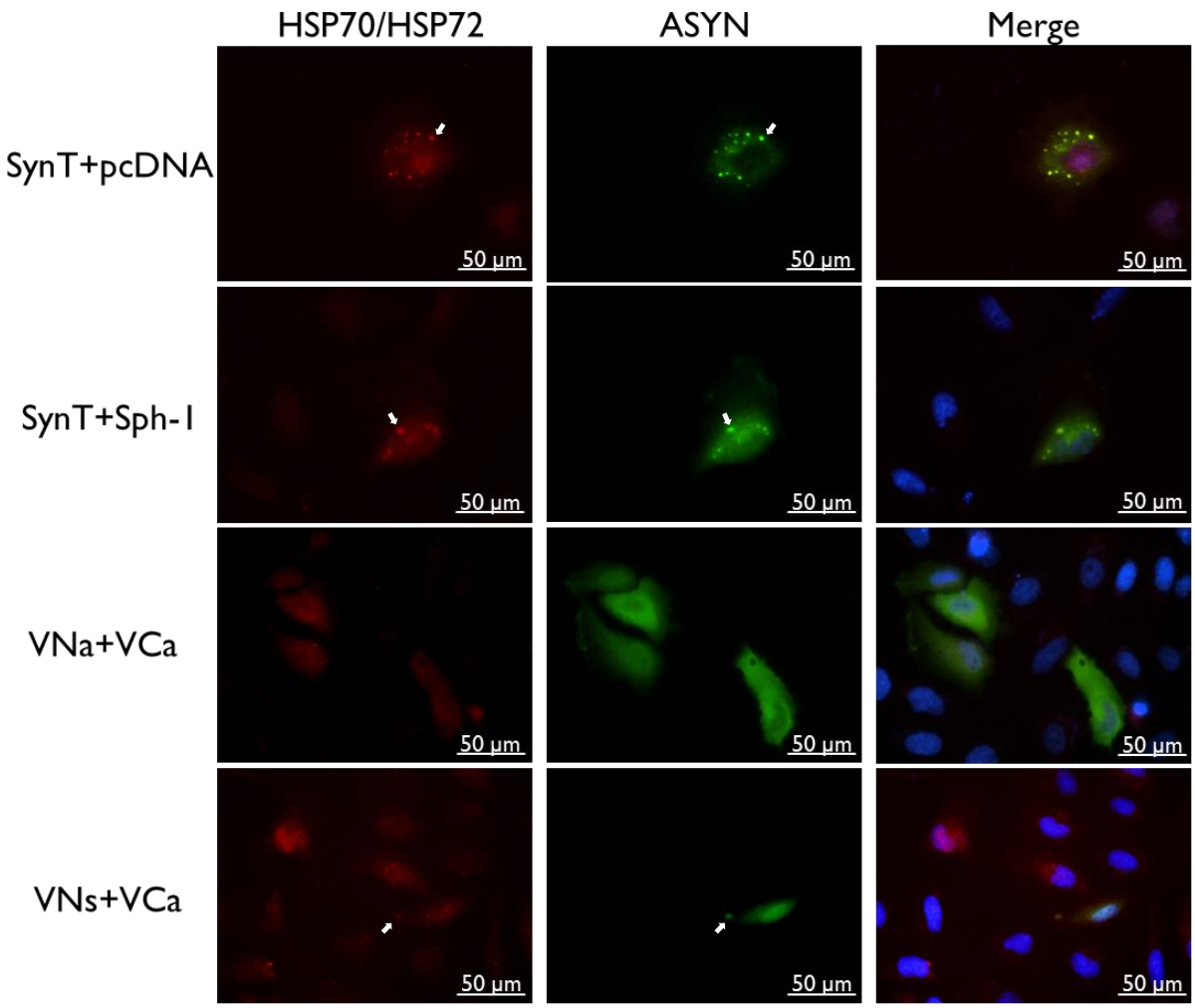

Figure 4.8 Co-localization studies of ASYN with HSP70. From the immunostaining of ASYN and HSP70 in H4 cells transfected with the SynT and BiFC models, co-localization is shown to occur in both SynT transfection models and also in the VNs+VCa model.

4.3.5 Ubiquitin co-localizes with ASYN inclusions in both synphilin-1 transfecting models

Ubiquitin is a protein responsible for leading misfolded proteins into the Ubiquitin-proteasome pathway for degradation. The dysfunction of this pathway in PD has been associated with the presence of ubiquitylated proteins in the Lewy Bodies, which would lead to a lack of free ubiquitin in the cytosol that would lead to a further increased occurrence of protein aggregation, making it a good candidate for this study [46, 47].

From the images obtained (Figure 4.9) it was possible to observe Ubiquitin co-localizing with ASYN in the VNs+VCa and SynT+sph1 transfection models, with the latter being peculiar in how it showcases what seems to be an ubiquitin inclusion which is surrounded by a layer of ASYN.

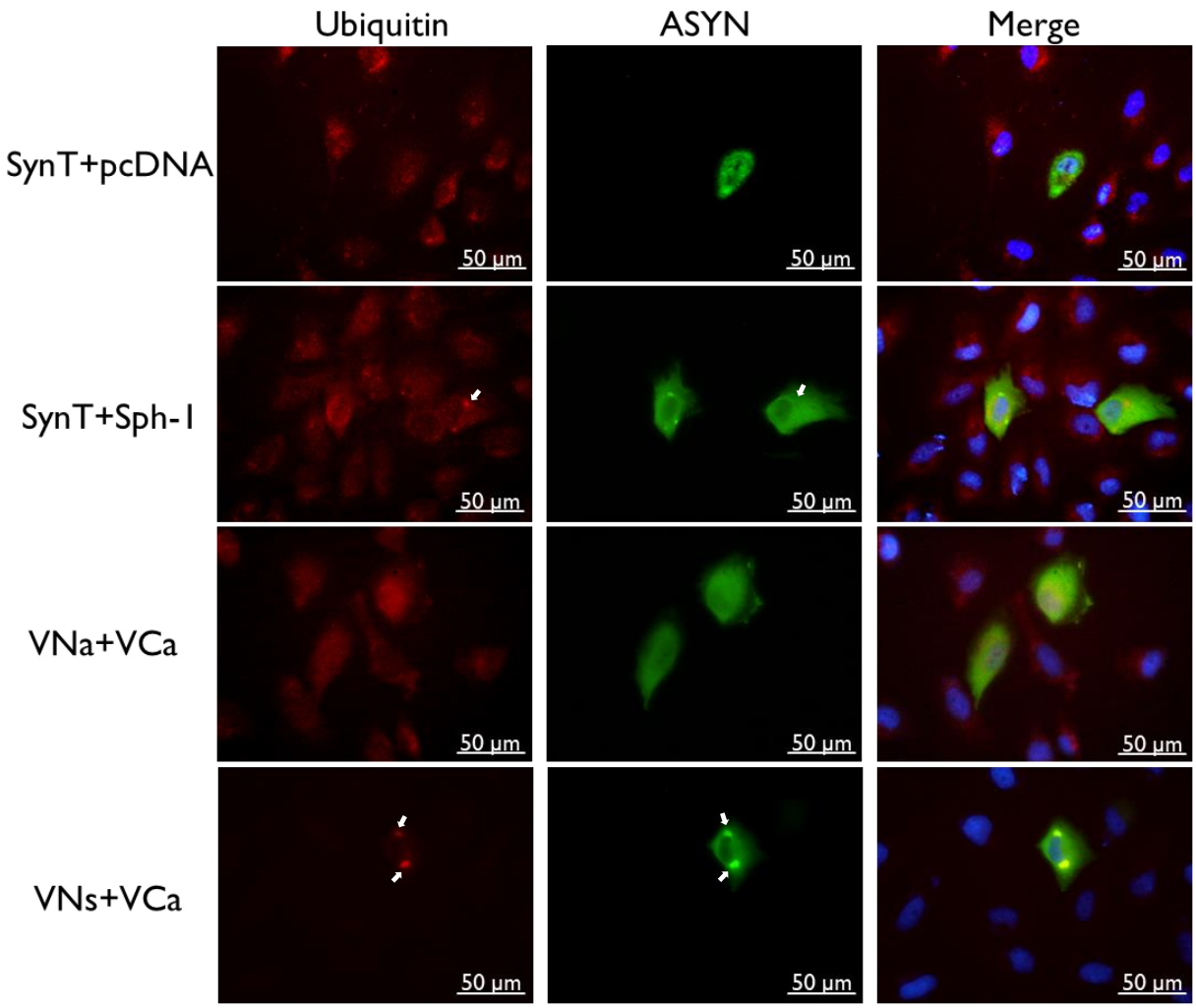

Figure 4.9 Co-localization studies of ASYN with Ubiquitin. From the immunostaining of ASYN and Ubiquitin in H4 cells transfected with the SynT and BiFC models, it is possible to observe co-localization of these proteins in the inclusions present at the sph-1 transfected cells.

4.4. STED microscopy and alternating display orientations on cells with the SynT transfection model

To further explore techniques for studying these heterogenous ASYN inclusions a study was done utilizing the SynT transfection model on H4 cells utilizing a super-resolution STED microscope.

Here, even without applying the STED beam to the cells, the images obtained (Figure 4.11) are still of a clear higher quality than the ones obtained from the previous fluorescence microscopes utilized, with the STED images showing a slight increase clarity in comparison to the confocal images, something that would be further improved with better optimization. The SynT+sph-1 transfected cells showcased ASYN showcasing inclusions and having a significant presence in the area of the nucleus, of which sph-1 seems mostly absent from. ASYN in the SynT+pcDNA transfected cells seems to be distributed in a similar fashion as with the other transfection model, with the main change being the decrease in inclusions, seemingly only presenting a single small noticeable inclusion. Meanwhile the v5-tag antibody seems to also be present (being distributed in the image as scattered small dots) despite the

apparent lack of sph-1 in the cells, alluding again to the antibody's possible lack of complete specificity to the v5-tag.

One feature that we experimented with in this microscope was the imaging of the cells while utilizing different display orientations (Figure 4.10). The ability to take images from these different orientations may allow for a better and more three-dimensional analysis of these heterogenous ASYN inclusions' structure and composition. This could even be further enhanced by applying the STED beam or even by utilizing the X10 ExM technique on the cells, although utilizing the STED beam may become problematic due to the bleaching of the fluorophores, which would be intensified by imaging the same section of a cell multiple times, limiting the number of times it can be used on a specific inclusion.

But overall, the STED microscopy technique can be an extremely valuable asset for the study of the contents of an inclusion.

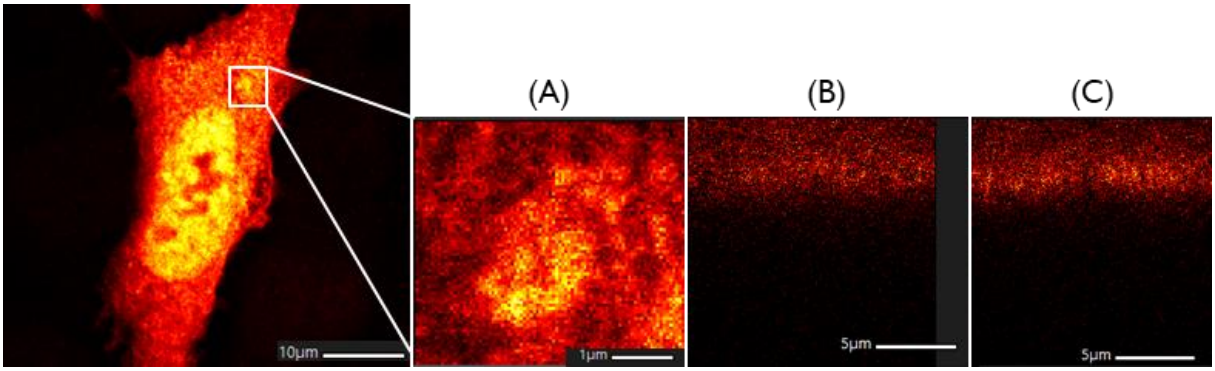

Figure 4.10 STED microscopy images of an inclusion utilizing three different display orientations. **(A)** Image of an ASYN inclusion taken at the YX display orientation. **(B)** Image of an ASYN inclusion taken at the YZ display orientation. **(C)** Image of an ASYN inclusion taken at the XZ display orientation.

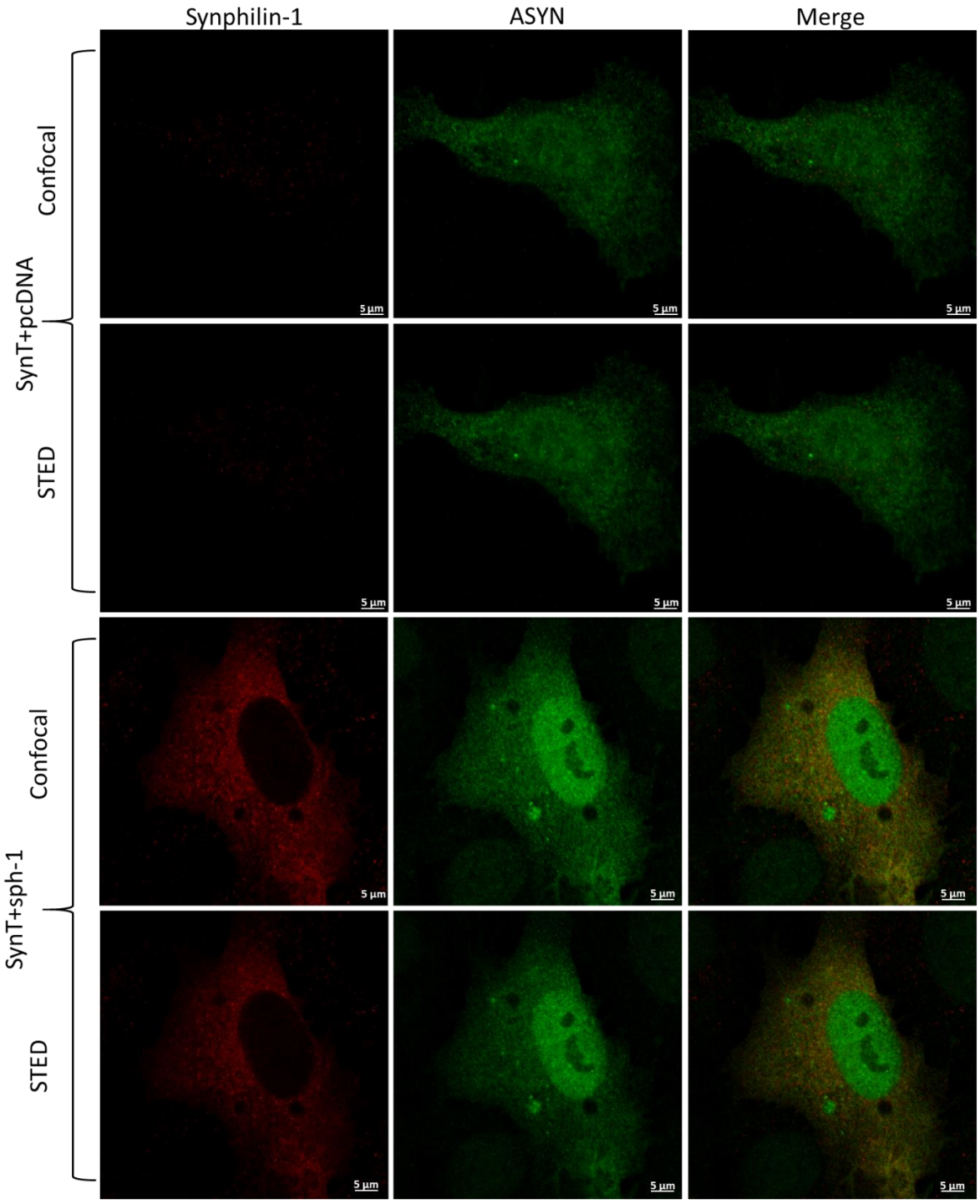

Figure 4.11 Comparison of images taken in a STED microscope with and without the STED beam of H4 cells transfected with the SynT model. These cells were immunostained for the ASYN (green) and synphilin-1 (red) proteins and the images were taking using a 100× objective.

5. Discussion

Neurodegenerative diseases have long been an enormous burden for the health of people worldwide, being generally difficult to discover treatments that could put an end to such pathologies. PD and DLB are two of the most common neurodegenerative diseases, and both of them possess LBs as one of their main histopathological hallmarks. Despite this, the molecular structure of LBs is still relatively unknown, and the impact that its presence has on neurons is still undetermined, whether it is helping to reduce neurodegeneration by grouping ASYN or doing the opposite through possible toxicity or by sequestering several different cellular molecules leading to a loss-of-function within the cells, or even just being inert. Therefore, discovering the architecture and function of the LBs could be imperative in understanding the exact way in which the presence of LBs has an effect on the neurodegeneration that occurs in these pathologies [3, 8, 10].

In this project we show how the established SynT and BiFC transfection models in H4 cells may be used as a model for the study of LB-like heterogenous ASYN inclusions and also how novel super-microscopy techniques (X10 Expansion microscopy and STED microscopy, specifically) bring a lot to the table in terms of their utilization for the analysis of the structure of LBs, or in the case of this study LB-like heterogenous ASYN inclusions.

5.1. The BiFC and SynT models allow the formation of LB-like heterogenous ASYN inclusions.

Throughout this project a focus was done on analyzing H4 cells that had been transfected with SynT and BiFC models. These were the transfection of VNa+VCa, which allows for the observance of ASYN oligomerization [19], and the transfection of SynT+pcDNA, SynT+sph-1 and VNs+VCa allowing for the imaging and study of ASYN inclusions (Figure 4.3), more so with the latter two transfections due to the usage of the inclusion-facilitating sph-1 [25]. This includes the study of large LB-like ASYN inclusions, with the SynT transfection model already being known to allow for the consistent formation of these inclusions in H4 cells [19, 22, 23, 48].

With the main objective of this project being the study of ASYN aggregation from a molecular perspective the focus became the analysis of co-localization between the ASYN protein and other proteins that have been found to be present in LBs, while utilizing the X10 expansion microscopy procedure in order to observe whether or not it was possible to obtain a good visualization of the presence of these protein in the heterogenous inclusions' architecture.

Unfortunately, due to the inability of imaging these cytoplasmic proteins after the X10 expansion microscopy procedure, it was not possible to obtain images that allowed the observance of the placement of these proteins in the structure of the ASYN inclusions (Figure 4.4), so the study on this area became limited to pre-expansion imaging of the cells.

Through imaging of the pre-expansion H4 cells it was at least still possible to observe that most of the proteins chosen show clear co-localization with ASYN's inclusions (Figures 4.5 to 4.9), with the exception of the mitochondrial protein TOM20, although it has already been shown in literature to be present in LB-like inclusions, showing that these proteins would be good avenues to further explore in terms of their part in the structure of LBs [3, 10, 49].

5.2. X10 microscopy can prove to be the future of widespread usage of super-resolution microscopy techniques.

Usage of ExM techniques to this day has been somewhat limited, given its novelty as a microscopy technique, with, at the time of writing, no published articles existing concerning its usage for studies related with PD or ASYN. Given the accessibility in utilizing this technique, and with the ability of certain variants (iExM and X10 ExM) of allowing for the imaging of cells and tissues that surpasses the boundaries on resolution that are set by the diffraction limit on even regular confocal microscopes [26], this technique shows a lot of promise in the possibilities that it opens for cheap and widespread usage of super-resolution microscopy.

Utilizing the X10 ExM technique on cells transfected with the SynT and BiFC models (Figure 4.3) (Figure 4.4) it was possible to better observe the distribution of free ASYN present in the cell's cytoplasm, showing them distributed in a punctuated form that resembles somewhat what was obtained from STED imaging (4.11). The technique also allowed for the observance of the heterogenous structure that is present in some of the larger ASYN inclusions that appear with these cell models, which seem to further showcase how these cell models can allow for the analysis of LB-like inclusions [19, 48]. Further analysis of the structure and composition of these inclusions could hopefully bring a better understanding of their role in LB-involved pathologies such as PD and DLB.

Given the main issue with the X10 ExM images obtained is the extremely low fluorescent signal observed in comparison with pre-expansion cells (Figure 4.4), this should be the first issue to be tackled. In literature there are several suggestions for actions that can be taken in order to mitigate this issue. This includes having longer incubation times with primary antibodies, further increasing the concentration of antibodies, or even performing an antigen retrieval step after fixating the cells with PFA and before the immunostaining. The samples could also be left with the anchoring solution for longer periods of time, and alternatively the immunostaining step could be performed post-expansion of the samples, although this last action can prove unpredictable due to the unknown state of the proteins' antigen structure after an expansion procedure [38].

Despite this loss of fluorescent signal intensity both the ASYN protein and the DAPI stained nucleus were still reliably observable through the Leica microscope (Figure 4.3) (Figure 4.4), although still having their fluorescent signal significantly reduced. One possibility for why this happens may be due to ASYN being transfected, which may lead to the protein being present in much higher quantities in the cells in comparison to the other proteins. Due to the expansion gels for cells immunostained for ASYN and sph-1 suffering problems during the gelation step it was unfortunately not possible to confirm whether sph-1 would be observable in cells with the SynT+sph-1 transfection model, warranting further study.

Another issue present with performing the X10 expansion microscopy procedure for imaging is the amount of time it can take from cell transfection to obtaining images of expanded cells, with the time needed to image the expanded cells being considerably higher due to the loss of fluorescent signal which the cells' detection and the adjustment of the focus due to the higher exposure times required. Besides this caveat there is also the time between cell transfection and imaging the expanded cells taking around, without counting a possible imaging of the cells before their expansion, 6 to 7 days. There are ways to shorten the time required for preparing the cells, like shortening the amount of time the cells are in contact with the antibody solutions, and also shortening the amount of time given for the gel to polymerize, but these tactics may come with a risk of poorer results when doing cell imaging.

Even with the aforementioned hurdles in the usage of this technique it still shows a lot of promise and could very well become the most widely used form of super-resolution microscopy given the relative low-cost in usage while still allowing for the achievement of resolutions off around 25 nm, which are comparable to the obtainable resolutions from other more expensive super-resolution techniques such as high end STED and STORM microscopy (which are around 20-30 nm), while also being much easier and less time-consuming to perform in comparison to iExM. The technique also has the advantage that, since it is only applied to the samples themselves and not involving the usage of specific microscopes, it can be mixed with other super resolution techniques, which would allow for resolutions much higher than what has ever been achievable before [26, 50, 51].

5.3. STED and Display orientation could be important tools in the study of heterogenous ASYN inclusions.

STED microscopy is another good candidate for the study of these heterogenous ASYN inclusions, allowing for the capture of very high-quality images that are able to surpass the diffraction limit of light microscopy, without necessitating the use of mathematical models to achieve it [29, 30]. The images obtained from cell models with SynT, although requiring further optimization to reach the full potential of the technique, showcase its ability of allowing for a clearer differentiation between close fluorophores (Figure 4.11). Optimization could be made in areas such as changing which lasers are being used and their intensity, and changing the size of the pixels in the obtained images (which dictates the area that the STED beam is applied to).

The usage of the display orientation settings in this microscope (Figure 4.10) also allowed for a more three-dimensional view of these ASYN inclusions, which can serve as an especially useful tool for the study of its structure. One downside is that its combined usage with STED could prove problematic due to the photobleaching of the sample's antibodies, so in future studies attempts could be made on utilizing it with samples that have gone through the X10 ExM procedure, to be able to achieve a similar resolution without requiring the usage of a STED beam [28].

5.4 Future avenues

Given that in this project the only type of cell used was H4 cell cultures, which lacks any sort of dopaminergic phenotype, a promising avenue to follow would be to attempt the application of the X10 expansion microscopy method and the SynT and BiFC transfection models with transfected dopaminergic primary culture neurons, in order to study these inclusions in a physiological setting, or even with immortalized cells differentiated to dopaminergic phenotype. Through this it will hopefully be possible to obtain a more accurate representation of the inclusions that would be found in people suffering from these pathologies, although these cells (especially the primary culture) would probably require a larger degree of optimization in order to be compatible with the X10 ExM procedure, in comparison to H4 cells [52].

Another possible future avenue to consider would be to combine both of these previously mentioned microscopy techniques, by applying the X10 microscopy procedure to a sample and then observing it through a super-resolution STED microscope, which would allow for a much greater amount of detail to be observable. However, the combination of these techniques might necessitate the usage of nanobody-based or small molecule tags, due to the distortion that can come from the size of the conventional antibodies, although there has not yet been developed any of these smaller tags that would

be compatible with the ExM technique [26, 36]. One thing to note is that it is still somewhat unknown the effect that the STED beam might have on the fluorophores considering their already decreased fluorescent signal, although there have already studies that have successfully combined the regular ExM technique with STED microscopy [17, 54]. For the combination of X10 ExM and STED to work, it will be required to develop probes for fluorescent labelling that are smaller than the conventional antibodies used and compatible with the ExM technique, in order to overcome image distortions that result from the size of antibodies in comparison to some subcellular structures. Through this it would become possible to further increase the resolution of these images with the combination of the X10 microscopy technique with other super-resolution microscopy techniques, and would possibly also allow the iExM technique to reach its full potential [26, 36].

For a better analysis of the inclusions, it could also prove advantageous to perform Z-Stacking of these cells models while also utilizing the aforementioned super-resolution microscopy techniques. Together with co-localization studies it could allow for the creation of 3D models of the inclusions in which it would be possibly to see exactly how ASYN and other cytoplasmic proteins are distributed throughout its structure.

All in all, through the usage of these super-resolution microscopy techniques it will hopefully be possible to perform highly detailed studies of these LB-like heterogenous ASYN inclusions that could lead us to a better understanding of their contents, structure and function, which may lead us a step further into figuring out what is their involvement with neurodegeneration in pathologies such as PD and DLB and how it could be interfered with in order to put an end to these pathologies..

6. References

[1] Gitler, A. D., Dhillon, P. & Shorter, J. Neurodegenerative disease: Models, mechanisms, and a new hope. *DMM Disease Models and Mechanisms* **10**, 499–502 (2017).

[2] Hartl, F. U. Protein misfolding diseases. *Annu. Rev. Biochem.* **86**, 21–26 (2017).

[3] Mahul-Mellier, A. L. *et al.* The process of Lewy body formation, rather than simply α-synuclein fibrillization, is one of the major drivers of neurodegeneration. *Proc. Natl. Acad. Sci. U. S. A.* **117**, 4971–4982 (2020).

[4] Balchin, D., Hayer-Hartl, M. & Hartl, F. U. In vivo aspects of protein folding and quality control. *Science* (2016).

[5] Ciechanover, A. Proteolysis: From the lysosome to ubiquitin and the proteasome. *Nature Reviews Molecular Cell Biology* **6**, 79–86 (2005).

[6] Cuervo, A. M. *et al.* Autophagy and aging: the importance of maintaining 'clean' cells. *Autophagy* **1**, 131–140 (2005).

[7] Krisko, A. & Radman, M. Protein damage, ageing and age-related diseases. *Open Biology* **9**, (2019).

[8] Marvian, A. T., Koss, D. J., Aliakbari, F., Morshedi, D. & Outeiro, T. F. In vitro models of synucleinopathies: informing on molecular mechanisms and protective strategies. *Journal of Neurochemistry* **150**, 535–565 (2019).

[9] Anderson, J. P. *et al.* Phosphorylation of Ser-129 is the dominant pathological modification of α-synuclein in familial and sporadic lewy body disease. *J. Biol. Chem.* **281**, 29739–29752 (2006).

[10] Wakabayashi, K. *et al.* The Lewy body in Parkinson's disease and related neurodegenerative disorders. *Molecular neurobiology* **47**, 495–508 (2013).

[11] Poewe, W. *et al.* Parkinson disease. *Nat. Rev. Dis. Prim.* **3**, 1–21 (2017).

[12] de Lau, L. M. & Breteler, M. M. Epidemiology of Parkinson's disease. *Lancet Neurology* **5**, 525–535 (2006).

[13] Devi, L. & Anandatheerthavarada, H. K. Mitochondrial trafficking of APP and alpha synuclein: Relevance to mitochondrial dysfunction in Alzheimer's and Parkinson's diseases. *Biochimica et Biophysica Acta - Molecular Basis of Disease* **1802**, 11–19 (2010).

[14] Ugalde, C. L. *et al.* Misfolded α-synuclein causes hyperactive respiration without functional deficit in live neuroblastoma cells. *DMM Dis. Model. Mech.* **13**, (2020).

[15] Ghio, S., Kamp, F., Cauchi, R., Giese, A. & Vassallo, N. Interaction of α-synuclein with biomembranes in Parkinson's disease - Role of cardiolipin. *Progress in Lipid Research* **61**, 73–82 (2016).

[16] Amer, D. A. M., Irvine, G. B. & El-Agnaf, O. M. A. Inhibitors of α-synuclein oligomerization and toxicity: A future therapeutic strategy for Parkinson's disease and related disorders. in *Experimental Brain Research* **173**, 223–233 (2006).

[17] Takeda, A. *et al.* Mechanisms of neuronal death in synucleinopathy. *Journal of Biomedicine and Biotechnology*, (2006).

[18] Outeiro, T. F. *et al.* Formation of toxic oligomeric α-synuclein species in living cells. *PLoS One* **3**, (2008).

[19] Lázaro, D. F. *et al.* Systematic Comparison of the Effects of Alpha-synuclein Mutations on Its Oligomerization and Aggregation. *PLoS Genet.* **10**, (2014).

[20] Ebrahimi-Fakhari, D. *et al.* Distinct roles in vivo for the Ubiquitin-Proteasome system and the Autophagy-Lysosomal Pathway in the Degradation of α-Synuclein. *J. Neurosci.* **31**, 14508–14520 (2011).

[21] Parihar, M. S., Parihar, A., Fujita, M., Hashimoto, M. & Ghafourifar, P. Alpha-synuclein overexpression and aggregation exacerbates impairment of mitochondrial functions by augmenting oxidative stress in human neuroblastoma cells. *Int. J. Biochem. Cell Biol.* **41**, 2015–2024 (2009).

[22] McLean, P. J., Kawamata, H. & Hyman, B. T. α-Synuclein-enhanced green fluorescent protein fusion proteins form proteasome sensitive inclusions in primary neurons. *Neuroscience* **104**, 901–912 (2001).

[23] Masaracchia, C. *et al.* Molecular characterization of an aggregation-prone variant of alpha-synuclein used to model synucleinopathies. *Biochim. Biophys. Acta - Proteins Proteomics* **1868**, (2020).

[24] Xie, Y.-Y. *et al.* Interaction with synphilin-1 promotes inclusion formation of α-synuclein: mechanistic insights and pathological implication. *FASEB J.* **24**, 196–205 (2010).

[25] Ribeiro, C. S., Carneiro, K., Ross, C. A., Menezes, J. R. L. & Engelender, S. Synphilin-1 is developmentally localized to synaptic terminals, and its association with synaptic vesicles is modulated by α-synuclein. *J. Biol. Chem.* **277**, 23927–23933 (2002).

[26] Truckenbrodt, S. *et al.* X10 expansion microscopy enables 25-nm resolution on conventional microscopes. *EMBO Rep.* **19**, (2018).

[27] Hell, S. W. & Wichmann, J. Breaking the diffraction resolution limit by stimulated emission: stimulated-emission-depletion fluorescence microscopy. *Opt. Lett.* **19**, 780 (1994).

[28] Vicidomini, G., Bianchini, P. & Diaspro, A. STED super-resolved microscopy. *Nature Methods* **15**, 173–182 (2018).

[29] Pujals, S., Feiner-Gracia, N., Delcanale, P., Voets, I. & Albertazzi, L. Super-resolution microscopy as a powerful tool to study complex synthetic materials. *Nature Reviews Chemistry* **3**, 68–84 (2019).

[30] Xu, J., Ma, H. & Liu, Y. Stochastic optical reconstruction microscopy (STORM). *Curr. Protoc. Cytom.* **2017**, 12.46.1-12.46.27 (2017).

[31] Paës, G., Habrant, A. & Terryn, C. Fluorescent nano-probes to image plant cell walls by super-resolution STED microscopy. *Plants* **7**, (2018).

[32] Tortarolo, G., Castello, M., Diaspro, A., Koho, S. & Vicidomini, G. Evaluating image resolution in stimulated emission depletion microscopy. *Optica* **5**, 32 (2018).

[33] Chen, F., Tillberg, P. W. & Boyden, E. S. Expansion microscopy. *Science (80-.).* **347**, 543–548 (2015).

[34] Chozinski, T. J. *et al.* Expansion microscopy with conventional antibodies and fluorescent proteins. *Nat. Methods* **13**, 485–488 (2016).

[35] Tillberg, P. W. *et al.* Protein-retention expansion microscopy of cells and tissues labeled using standard fluorescent proteins and antibodies. *Nat. Biotechnol.* **34**, 987–992 (2016).

[36] Chang, J. B. *et al.* Iterative expansion microscopy. *Nat. Methods* **14**, 593–599 (2017).

[37] Asano, S. M. *et al.* Expansion Microscopy: Protocols for Imaging Proteins and RNA in Cells and Tissues. *Curr. Protoc. Cell Biol.* **80**, (2018).

[38] Truckenbrodt, S., Sommer, C., Rizzoli, S. O. & Danzl, J. G. A practical guide to optimization in X10 expansion microscopy. *Nat. Protoc.* **14**, 832–863 (2019).

[39] Tsai, Y. C., Riess, O., Soehn, A. S. & Nguyen, H. P. The Guanine Nucleotide Exchange Factor Kalirin-7 Is a Novel Synphilin-1 Interacting Protein and Modifies Synphilin-1 Aggregate Transport and Formation. *PLoS One* **7**, (2012).

[40] Di Maio, R. *et al.* α-synuclein binds to TOM20 and inhibits mitochondrial protein import in Parkinson's disease. *Science Translational Medicine* **8**, (2016).

[41] Suzuki, Y., Jin, C., Iwase, T. & Yazawa, I. β-III tubulin fragments inhibit α-synuclein accumulation in models of multiple system atrophy. *J. Biol. Chem.* **289**, 24374–24382 (2014).

[42] Walther, T. C. & Farese, R. V. Lipid droplets and cellular lipid metabolism. *Annu. Rev. Biochem.* **81**, 687–714 (2012).

[43] Alza, N. P., Iglesias González, P. A., Conde, M. A., Uranga, R. M. & Salvador, G. A. Lipids at the crossroad of α-synuclein function and dysfunction: Biological and pathological implications. *Frontiers in Cellular Neuroscience* **13**, (2019).

[44] Leverenz, J. B. *et al.* Proteomic identification of novel proteins in cortical Lewy bodies. *Brain Pathol.* **17**, 139–145 (2007).

[45] Leak, R. K. Heat shock proteins in neurodegenerative disorders and aging. *Journal of Cell Communication and Signaling* **8**, 293–310 (2014).

[46] Lowe, J. *et al.* Ubiquitin is a common factor in intermediate filament inclusion bodies of diverse type in man, including those of Parkinson's disease, Pick's disease, and Alzheimer's disease, as well as Rosenthal fibres in cerebellar astrocytomas, cytoplasmic bodies in muscle, and mallory bodies in alcoholic liver disease. *J. Pathol.* **155**, 9–15 (1988).

[47] Yerbury, J. J. *et al.* Walking the tightrope: Proteostasis and neurodegenerative disease. *Journal of Neurochemistry* **137**, 489–505 (2016).

[48] Burré, J., Sharma, M. & Südhof, T. C. Cell biology and pathophysiology of α-synuclein. *Cold Spring Harb. Perspect. Med.* **8**, (2018).

[49] Outeiro, T. F. *et al.* Small heat shock proteins protect against α-synuclein-induced toxicity and aggregation. *Biochem. Biophys. Res. Commun.* **351**, 631–638 (2006).

[49] Burré, J., Sharma, M. & Südhof, T. C. Cell biology and pathophysiology of α-synuclein. *Cold Spring Harb. Perspect. Med.* **8**, (2018).

[50] Zwettler FU, Reinhard S, Gambarotto D, Bell TDM, Hamel V, Guichard P, Sauer M. Molecular resolution imaging by post-labeling expansion single-molecule localization microscopy (Ex-SMLM). Nat Commun. 2020 Jul 7;11(1):3388. doi: 10.1038/s41467-020-17086-8. PMID: 32636396; PMCID: PMC7340794.

[51] Gambarotto, D. *et al.* Imaging cellular ultrastructures using expansion microscopy (U-ExM). *Nat. Methods* **16**, 71–74 (2019).

[52] Delenclos, M. *et al.* Cellular models of alpha-synuclein toxicity and aggregation. *Journal of Neurochemistry* **150**, 566–576 (2019).